Drone impact damage assessment on a legacy transport aircraft structure: empennage testing

Dadouche, Azzedine; Galeote, Brian; Breithaupt, Timothy; Greer, Allan; Gould, Ron

Laboratory Technical Report (National Research Council of Canada. Aerospace Research Centre. Gas Turbine Laboratory); no. LTR-GTL-2021-0002, 2021-01-18

Drone Impact Damage Assessment on a Legacy Transport Aircraft Structure: Empennage Testing

Report No: LTR-GTL-2021-0002

Prepared for: Defence Research and Development Canada

Authors:

NRC

Azzedine Dadouche
Brian Galeote
Timothy Breithaupt
Allan Greer

External

Ron Gould

Aerospace Research Centre, Gas Turbine Laboratory

January 18, 2021

National Research Council Canada
Conseil national de recherches Canada

Canada

Contents

1 INTRODUCTION

The Gas Turbine Laboratory of NRC's Aerospace Research Centre has an extensive experience in impact testing on aircraft structures, windshields as well as on engines (bird ingestion). A number of pneumatic guns with various sizes have been developed to perform such tests depending on the requirements.

Over the last two years and in collaboration with Transport Canada and Defence Research and Development Canada, the National Research Council Canada has developed a 17" bore cannon and completed two series of drone impact tests. The first series of impact tests was on aluminum plates [1] whereas, the second was on windshield and wing leading edge of a typical AWM 525 (Part 25) aircraft [2].

This is a follow-up project with the objective to perform a series of experiments simulating impacts between a representative quadcopter drone and the empennage of a transport category aircraft operating at typical cruising speed under 3,048 m (10,000 feet).

Test articles (empennage segments) were provided to NRC by the Emergency Response Services of the Ottawa International Airport Authority having been removed by NRC from one of their training aircrafts. This legacy aircraft served as a commercial passenger transporter until 1999 before being converted into a freighter. The plane was withdrawn from use in 2003 after 27 years of service.

There are several configurations of the empennage for transport category aircrafts with the most popular are conventional, cruciform and T-tail shapes. Having the location of the horizontal stabilizer and the wing on different planes, puts both parts at the same risk level of colliding with a bird or a drone. **Figure 1** presents pictures of aircrafts from various airframe manufacturers with distinct empennage configurations.

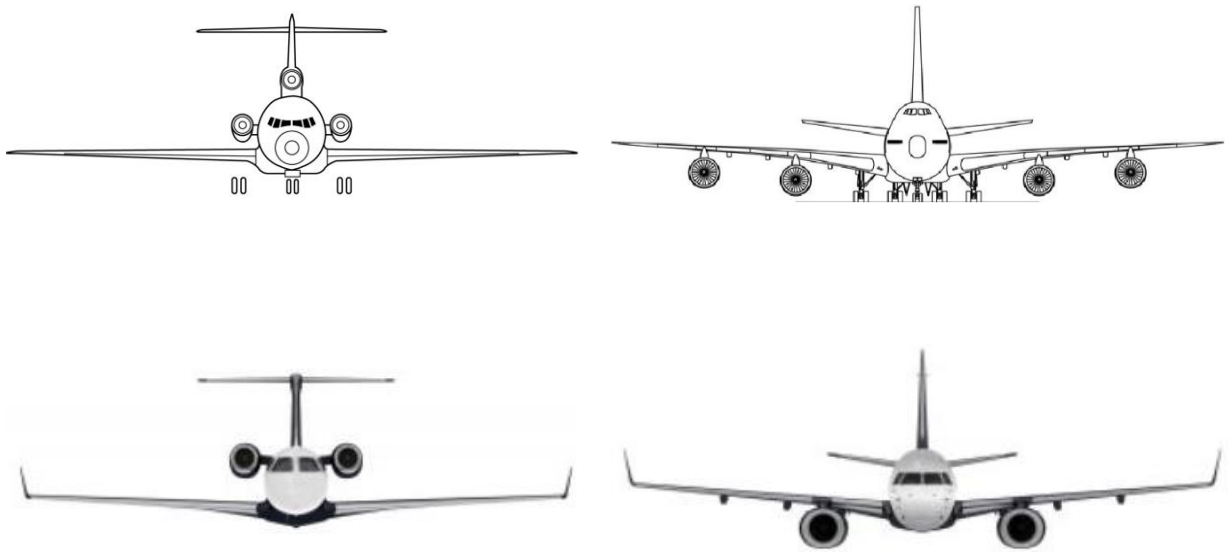

Figure 1: Common empennage configurations

2 EXPERIMENTAL SETUP

2.1 Drone cannon

An overall view of drone cannon is presented in **Figure 2**. It is composed of three main sections: pressure vessel, high-speed valve and a 17" stainless steel barrel. A guide rail runs along the 6 m (20 ft) barrel's bore and fits into a slot in the sabot sidewall to prevent rotation during acceleration.

Important note: Whenever LHS or RHS is used, it is always from an aircraft reference frame (i.e. when sitting inside the cabin facing forward).

Figure 2: General view of the drone super cannon

2.2 Test articles

The test empennage had a "T" shape. It was removed from the aircraft discussed in the Introduction section. Due to its 10.9 m (35'9") span and 4.4 m (14.5 ft) height, the empennage assembly was portioned into three parts (**Figure 3**) to facilitate transportation and fixturing. The cut lines on the left hand side (LHS) and right hand side (RHS) horizontal stabilizers (HS) were

parallel to the ribs. The elevators and trailing edge structure were trimmed back to the rear spar. The vertical stabilizer (VS) was trimmed to allow for handling and set up at the impact test facility (**Figure 4**). In this figure, the leading edge ribs (LER) on the HS were numbered for identification purposes. The two-piece rudder was completely removed and the remaining structure trimmed to a height of 2.74 m (9 ft) to bring down the total mass of the central part to 1300 kg (2,866.5 lb).

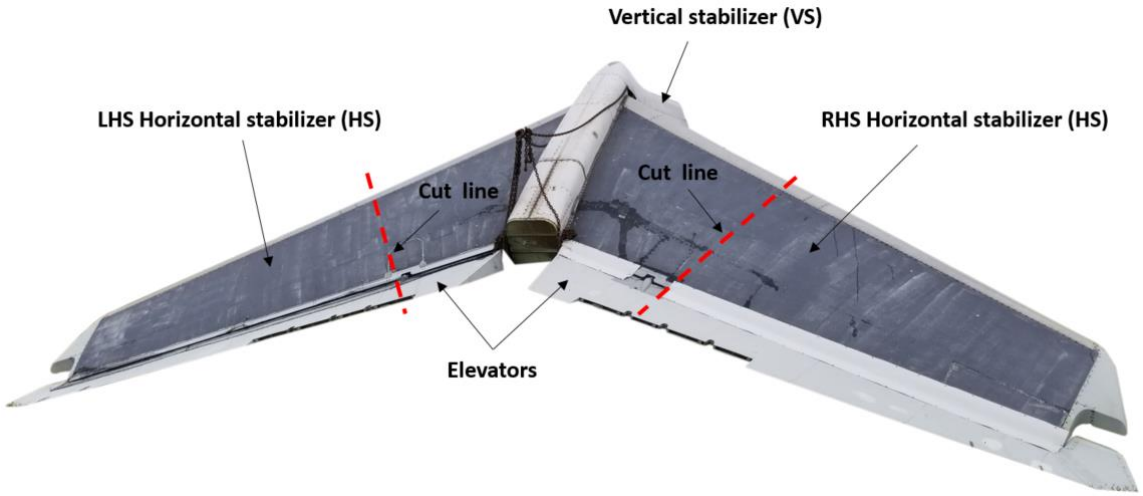

Figure 3: Test empennage

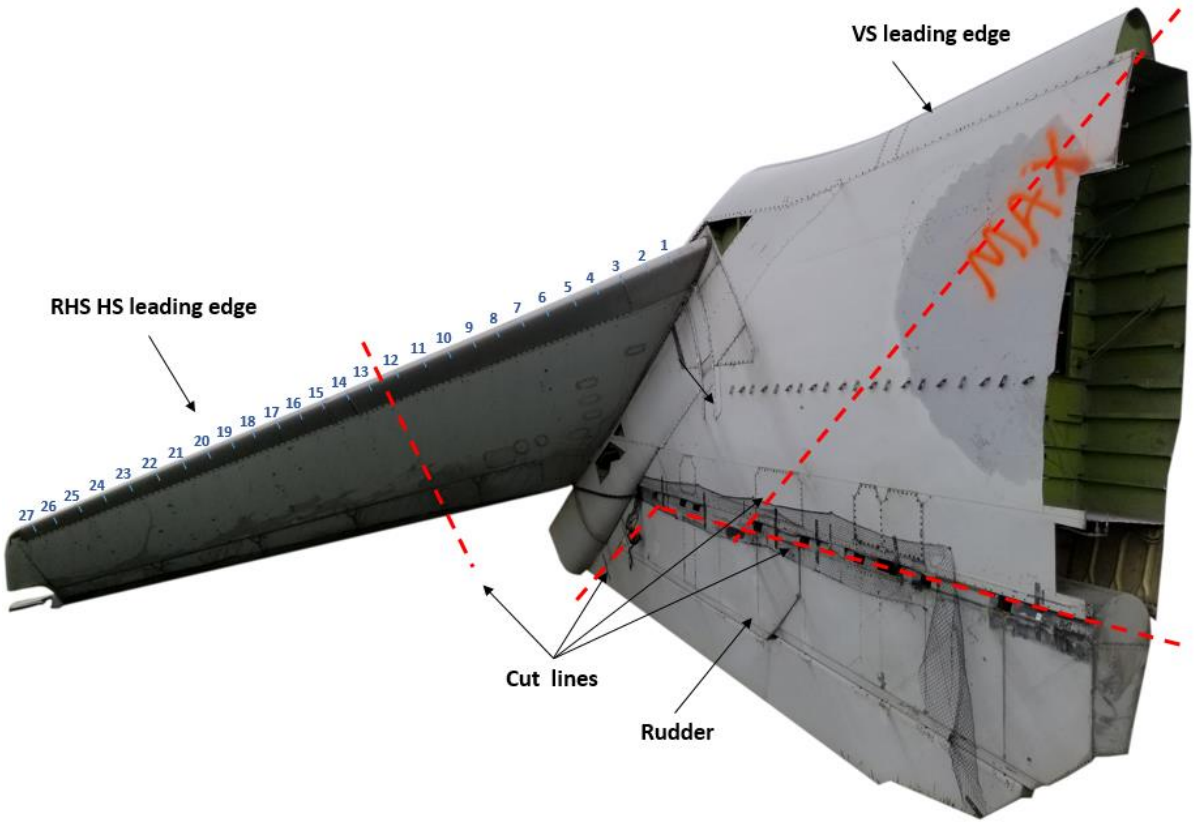

Figure 4: Cut lines on the vertical and RHS horizontal stabilizers

Figure 5 depicts the three test segments of the empennage under investigation. The central segment includes the vertical stabilizer and inboard portions of the horizontal stabilizers. All three segments are presented in an upside down position.

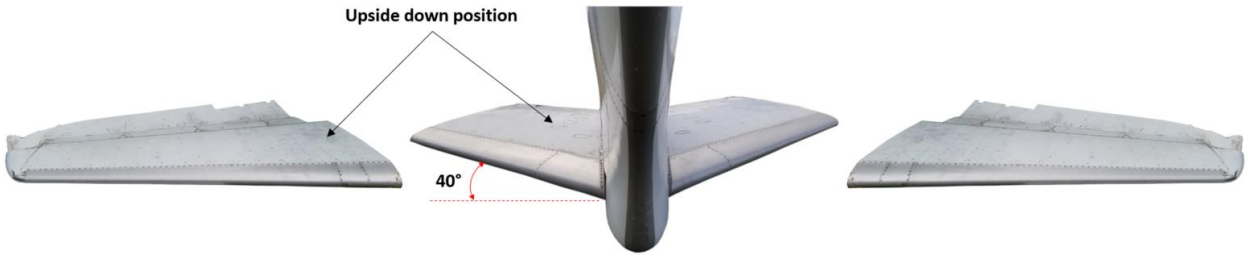

Figure 5: Test segments of the empennage

For consistency purposes, the same drone type and model used on the leading edge and windshield impact tests [2] was used for the empennage testing. Details of the drone are presented in **Table 1**.

Table 1. Drone details

Type	Model	Dimensions [mm, in]	Mass [kg, lb]
Full UAS	Quadcopter	192x287x287 7.56x11.31x11.31	1.2, 2.6

2.3 Test protocol

A total of seven drone impact tests were conducted: five tests on the horizontal stabilizer (HS) and two tests on the vertical stabilizer (VS). Three out of the five HS tests (HS-T1, HS-T2 and HS-T3) were performed on the outboard segment. **Figure 6** depicts some structural and dimensional details of the RHS tip segment presented in an upside-down position. The figure also identifies the impact locations of the first three tests (conducted on the LHS HS). The other two tests (HS-T4 and HS-T5) were performed on the inboard segment of the LHS HS as depicted in **Figure 7**. The figure also shows the impact location on the vertical stabilizer (VS-T10.

It is important to mention that the test segments were secured in place using heavy duty straps to prevent large and unpredictable displacement of the test articles after impact. Such constrains might not fully represent real boundary conditions but they allow securing the test segments in place. Additional details are given in section 3 for each test.

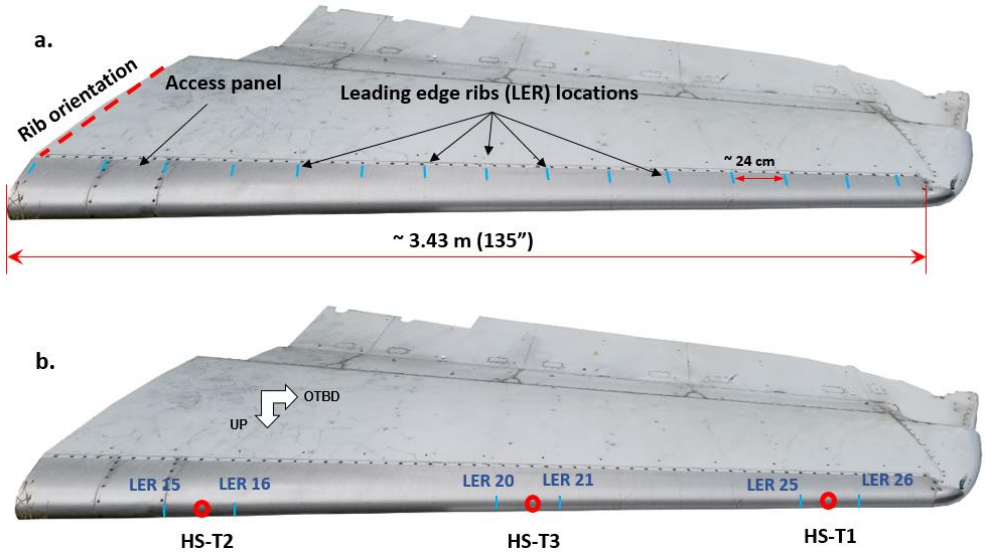

Figure 6: Tip segment of RHS HS (shown upside-down)

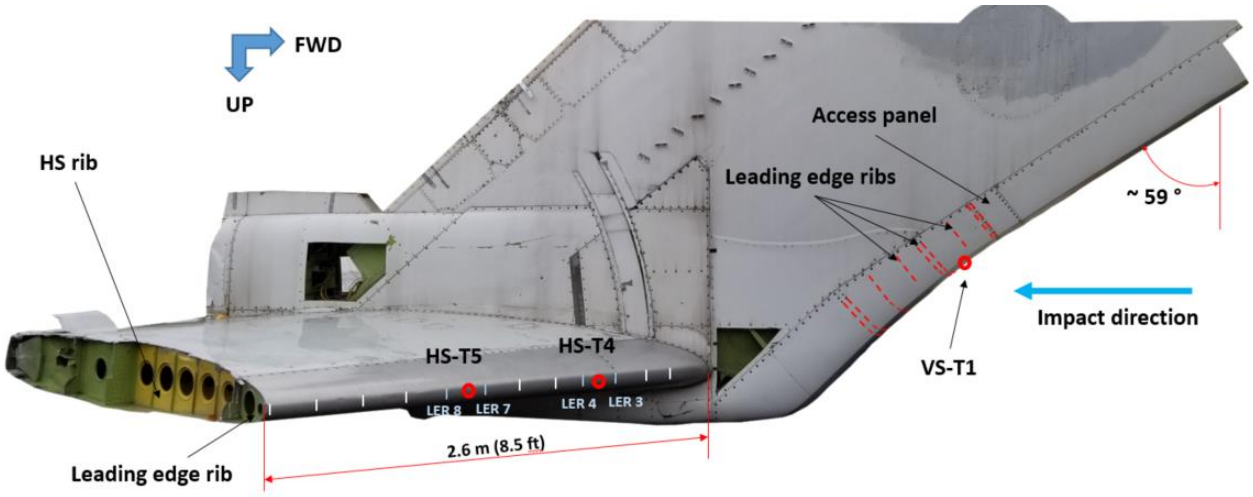

Figure 7: Empennage central segment (shown upside down)

The empennage under test features a sweep angle of 40° (HS) and a layback angle of 59° (VS) as shown in **Figure 8**. All tests conducted on the central segment (**Figure 7**) respected the actual sweep and layback angles of the empennage. This segment was set up in an upside-down configuration to ease fixturing and accommodate the cannon barrel height. For the tests conducted on the tip segment (**Figure 6**), the HS sweep angle was set to 32° to study its effect on damage severity level.

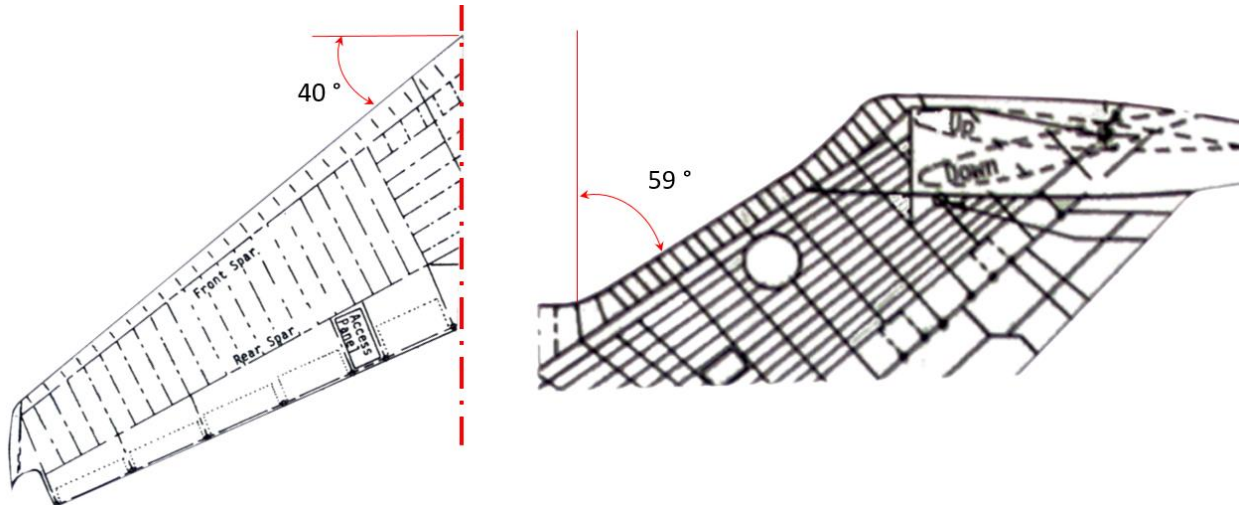

Figure 8: Sweep and layback angles of the HS and VS

Another test using a bird carcass was performed on the right hand side (RHS) horizontal stabilizer (HS-T6) as shown in **Figure 9**. The carcass was supplied to NRC by a local farm. This test was performed using a smaller bore pneumatic cannon in accordance with ASTM standard F330-16 [3]. The main objective of this test was to qualitatively assess the damage incurred to the leading edge of the HS and compare the damage severity level with the impact tests performed using the quadcopters.

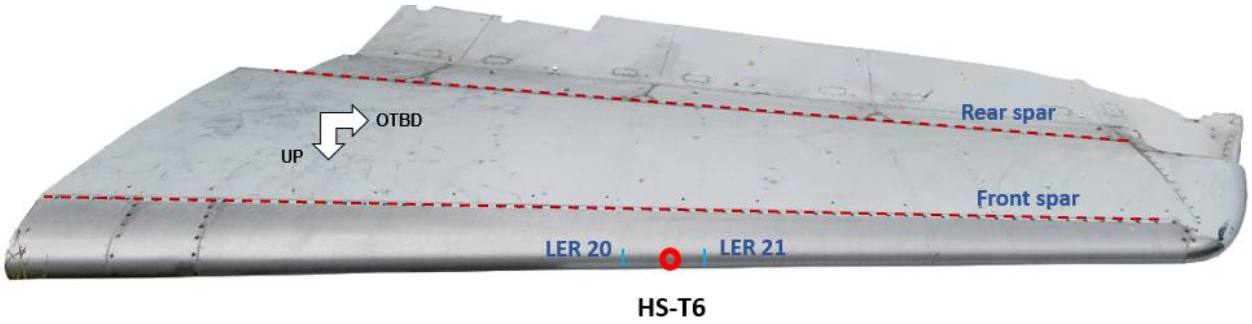

Figure 9: Location on the RHS HS tip segment for the bird impact test

The impact speed of the projectile and various angles were measured using high speed cameras (Mega Speed MS70K, MS90K, and MS120K). The cameras have also provided details of the impact sequence for each test at a rate of 4000 frames per second.

NRC's foam-based, split, "BAAT[i]" sabot was used to perform the impact tests [1]. All drone camera modules were zip-tied to their mounting pad on the drone to reduce the risk of separation during acceleration. **Figure 10** depicts a typical test drone without propeller blades. The four motors were identified by number and will be referred to as such in the data discussion section.

Table 2 gives details for each impact test. The speed of 250 knots was selected in accordance with the current regulations for aircraft operation under 10,000 feet [4]. It is also worth noting that the original plan was to conduct 50% of the tests using drones equipped with discharged batteries (<25%) and 50% of the tests using drones with fully charged batteries to assess the risk of fire. However, after the completion of Test #3, the project team decided to perform all remaining tests using drones with discharged batteries as the risk of fire was high and generation/spread of toxic fumes within the test facility was uncontrollable. This will be discussed further in section (3.1.3).

Table 2. Test matrix

Test #	Projectile	Weight, kg (lb)	Velocity		Target	Sweep angle (°)	Battery condition
			m/s	knots			
1	Quadcopter	1.2 (2.6)	128.6 (±2.5)	250 (±5)	LHS HS, tip (HS-T1)	32	Discharged (<25%)
2	Quadcopter	1.2 (2.6)	128.6 (±2.5)	250 (±5)	LHS HS, (HS-T2)	32	Discharged (<25%)
3	Quadcopter	1.2 (2.6)	128.6 (±2.5)	250 (±5)	LHS HS, middle (HS-T3)	32	Charged (100%)
4	Quadcopter	1.2 (2.6)	128.6 (±2.5)	250 (±5)	LHS HS, root (HS-T4)	40	Discharged (<25%)
5	Quadcopter	1.2 (2.6)	128.6 (±2.5)	250 (±5)	LHS HS, middle (HS-T5)	40	Discharged (<25%)
6	Quadcopter	1.2 (2.6)	128.6 (±2.5)	250 (±5)	VS (VS-T1)	59 (layback)	Discharged (<25%)
7	Bird carcass	1.2 (2.6)	128.6 (±2.5)	250 (±5)	RHS HS, middle (HS-T6)	32	N/A

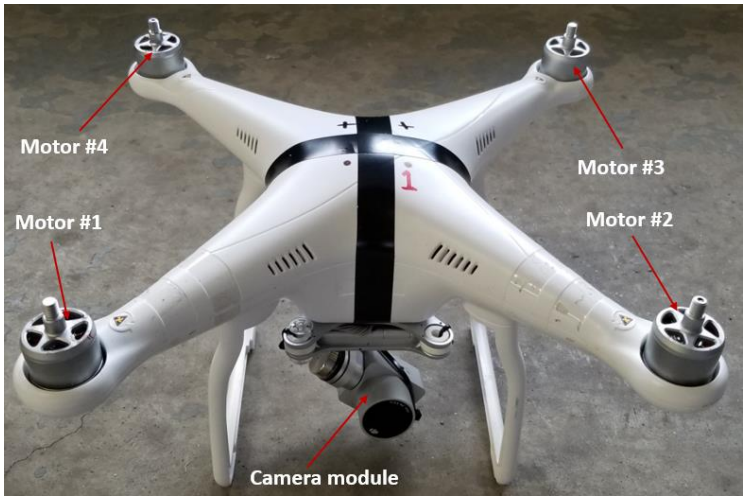

Figure 10: Typical quadcopter without rotor blades

3 DATA ANALYSIS AND DISCUSSION

The analysis of the experimental results is organized by test component article and projectile type. At first, the drone impacts on the horizontal stabilizer will be discussed. Then, impact results on the vertical stabilizer will be presented. The bird carcass strike on the horizontal stabilizer will be discussed last. A summary of the test campaign will also be given at the end of this section.

3.1 Drone impact on horizontal stabilizer

3.1.1 Test #1 (HS-T1)

The setup for the first test on the LHS HS is presented in **Figure 11**. The HS was setup at a 32° sweep angle. Four adjustable stands, secured to a steel plate were used to locate the HS at the appropriate height and orientation to the cannon. In addition to height adjustment, each stand features a pivoting flat plate and a rubber pad to match the curvature of the HS lower surface and ensure a soft and full contact. Heavy duty straps were also used to secure the test segment in place. The HS was sandwiched between the rubber pads and the straps. The latter were anchored to the steel plate via swivel hoist rings and tension was applied using a ratchet mechanism to secure the HS in place as shown in **Figure 11**. Even though this doesn't fully represent the exact boundary condition of the horizontal stabilizer on the aircraft, more than 45% (1.8 m, 5.9 ft) of the test segment was overhung to allow for movement as a result of the impact. In a real case, the whole length of the HS (5.6 m, 18.5 ft) will be overhung. An in-flight drone collision may lead to the generation of a temporary moment on the mechanism that actuates the position of the horizontal stabilizer. This is beyond the scope of this investigation and will not be discussed further.

Figure 11: LHS HS setup for tip test (HS-T1)

Figure 12 depicts the positions of the high speed cameras. The C2 camera was set perpendicular to the trajectory of the drone and allowed for the measurement of the impact speed as well as an estimation of the drone's pitch angle. C3 camera provided a front view of the leading edge and allowed an estimation of the drone roll angle. Camera C4 was pointed towards the muzzle of the cannon to visualize any issues with the sabot upon exiting the barrel. The successful sabot separation in the two first tests allowed the re-orientation of this camera towards the target

on the HS to capture the impact sequence. Another camera (C1) was installed in the ceiling above the HS looking straight down (not shown in the figure). This camera view allowed for the determination of the yaw angle as well as a second measurement of the impact speed.

Figure 12: High speed digital camera positions

Figure 13 shows the sequence of images from Test #1 (HS-T1) of the drone impact with the horizontal stabilizer at a recorded speed of 128.2 m/s (249.2 kt). During this first test, the drone experienced an upward pitch angle of 18°. However, the yaw and roll angles were insignificant with approximate values of 5.5° and 2° respectively. The relatively high pitch angle caused the motors M1 and M2 to miss the HS leading edge. However, the shot was on target. The main body and legs of the drone impacted the HS first followed by the motors M3 and M4 respectively. While the main body and battery pack penetrated through the leading edge, M3 and M4 each caused damage and fell on to the ground as a result of the breakage of their arms. The drone camera module did not contribute to the impact as it snapped off its mount before the impact and passed under the HS.

Selected pictures of the leading edge after the impact are presented in **Figure 14**. The impact resulted in an opening in the leading edge measuring 15.2x10.1x10.1 cm (6x4x4 inch), significant damage to the LER 26 and caused damage to the front spar and rib. Defective parts of the drone body and battery pouches landed at the back of the HS close to the rear spar as depicted in bottom pictures of **Figure 14**. Motor M3 damaged the LER 26, deformed the skin of the leading edge and caused a 5 cm (2 inch) long tear (**Figure 14d**). M4 was the last part of the drone to impact the HS causing a deep and extended deformation to the skin.

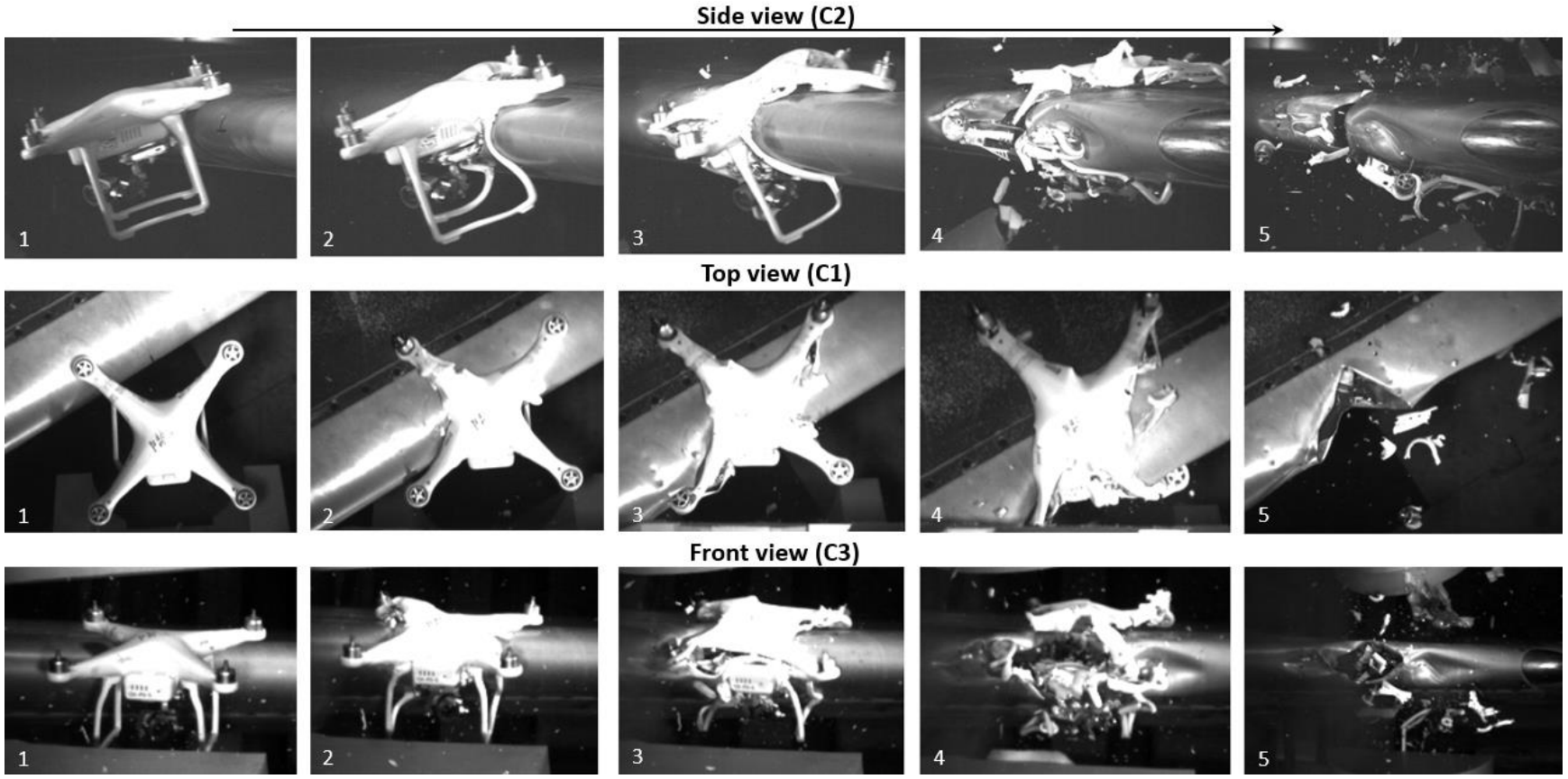

Figure 13: Drone/HS impact sequence (Test #1: HS-T1)

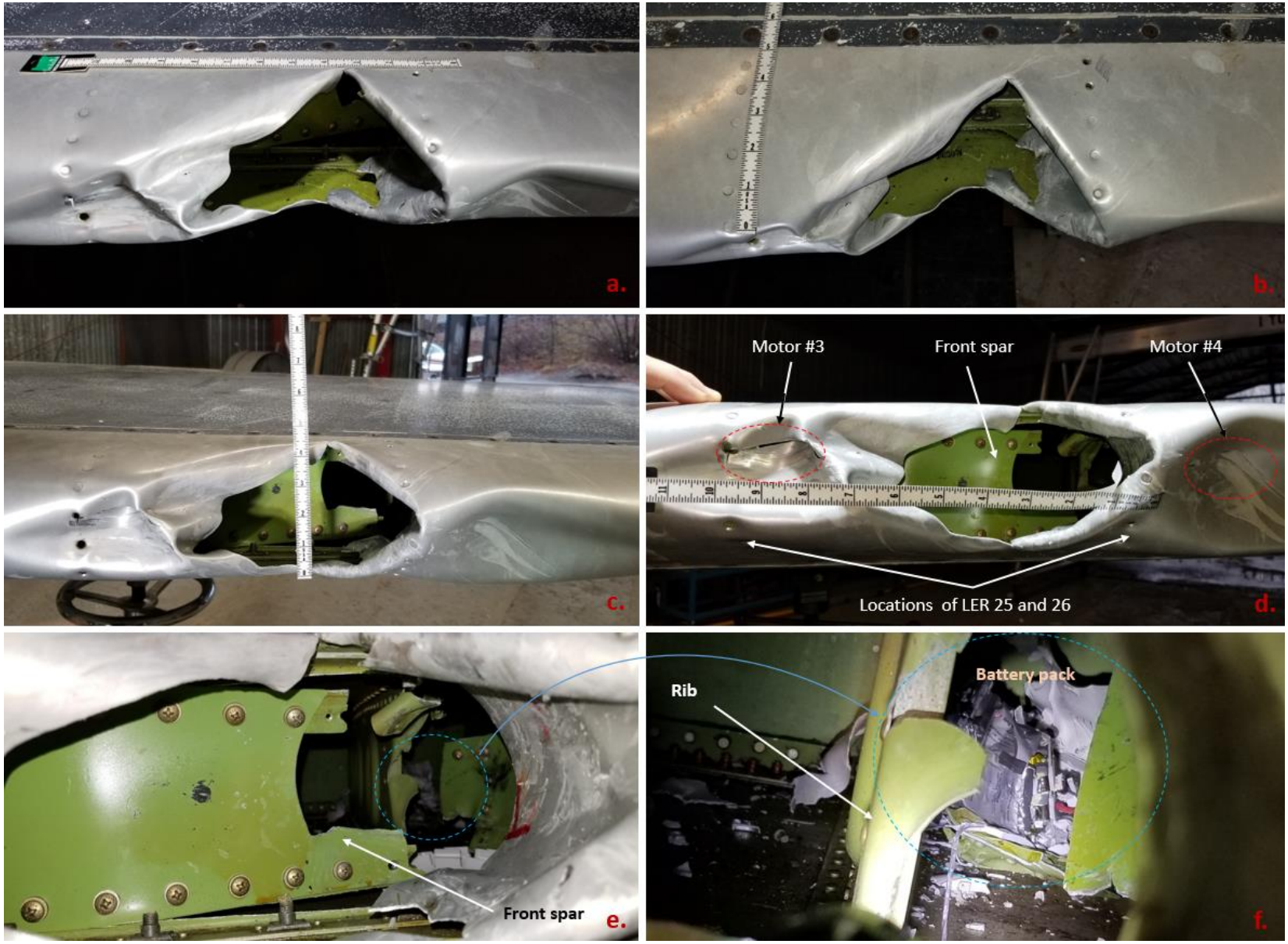

Figure 14: Pictures of damaged HS leading edge (Test #1: HS-T1)

It is important to note that the test drone had a discharged battery (under 25% of full charge). During inspection after the test, a very slight burning smell was reported. However, after extracting the battery cells from the back of the HS, the cells continued overheating and generating smoke and fumes as depicted in **Figure 15**. This was the direct effect of mechanical deformation of the battery assembly as well as its manipulation during extraction from the horizontal stabilizer. This may have caused a short circuit and ignition of the cells.

Figure 15: Status of the drone battery after impact

3.1.2 Test #2 (HS-T2)

The second test (HS-T2) was conducted on the inboard side of the LHS HS test segment between LER 15 and LER 16 as depicted in **Figure 16**. The same fixturing and restraint mechanism was used with a re-arrangement of the locations of the straps. It is important to note that the thickness of the leading edge in this area is much higher compared to that at its outboard side. In addition, LER 15 is stiffer and wider to allow the mounting of the leading edge skin with rivets on one side and an access panel on the other side with screws. A drone with a discharged battery was used for this test.

The shot was on target with a recorded impact speed of 126.4 m/s (245.7 kt) and resulted in a drone penetration into the leading edge. **Figure 17** shows frames extracted from the high speed camera videos. As opposed to the first test, the drone headed towards the target with a downward pitch angle of 9.5°. This resulted in a full impact by motors M1 and M2 with the leading edge. The yaw and roll angles were very limited with rotations of 5.5° and 5° respectively. Because of the HS sweep angle, the drone first hit the leading edge with motor M2, followed by M1 and then the main body. Motors M3 and M4 were the last to impact the leading edge as is clearly shown by the side view pictures. While motors M1, M2 and M3 penetrated the HS along with the battery pack, motor M4 punctured the leading edge and then deflected away as noted in the pictures extracted from the various high speed camera videos. The drone-mounted camera module missed the impact and continued its trajectory under the HS. Frames #2 and #3 of the C2 side view video show the drone camera as it passes under the HS.

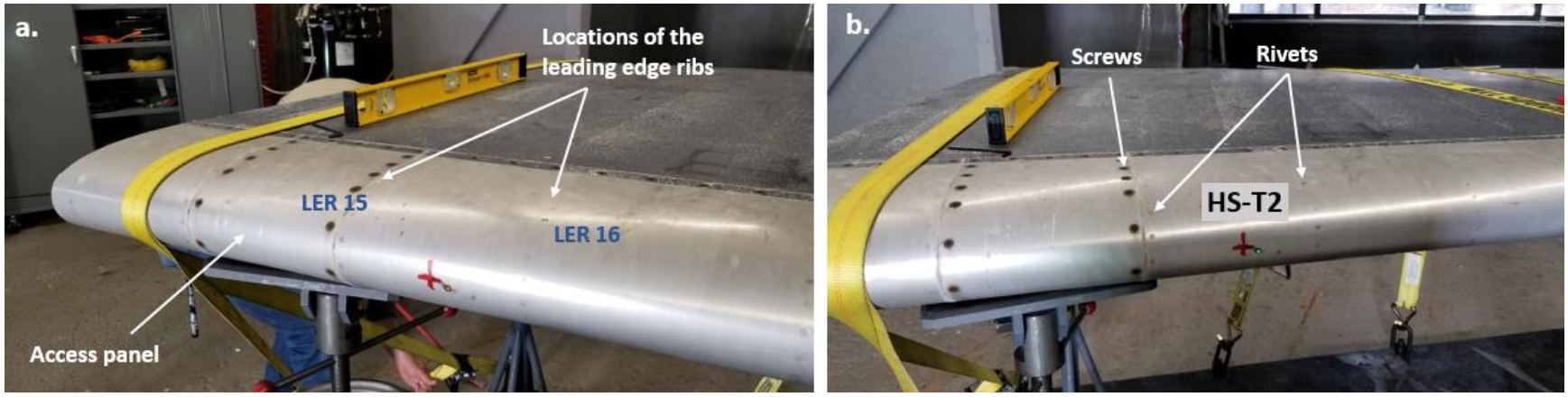

Figure 16: Test setup for HS-T2

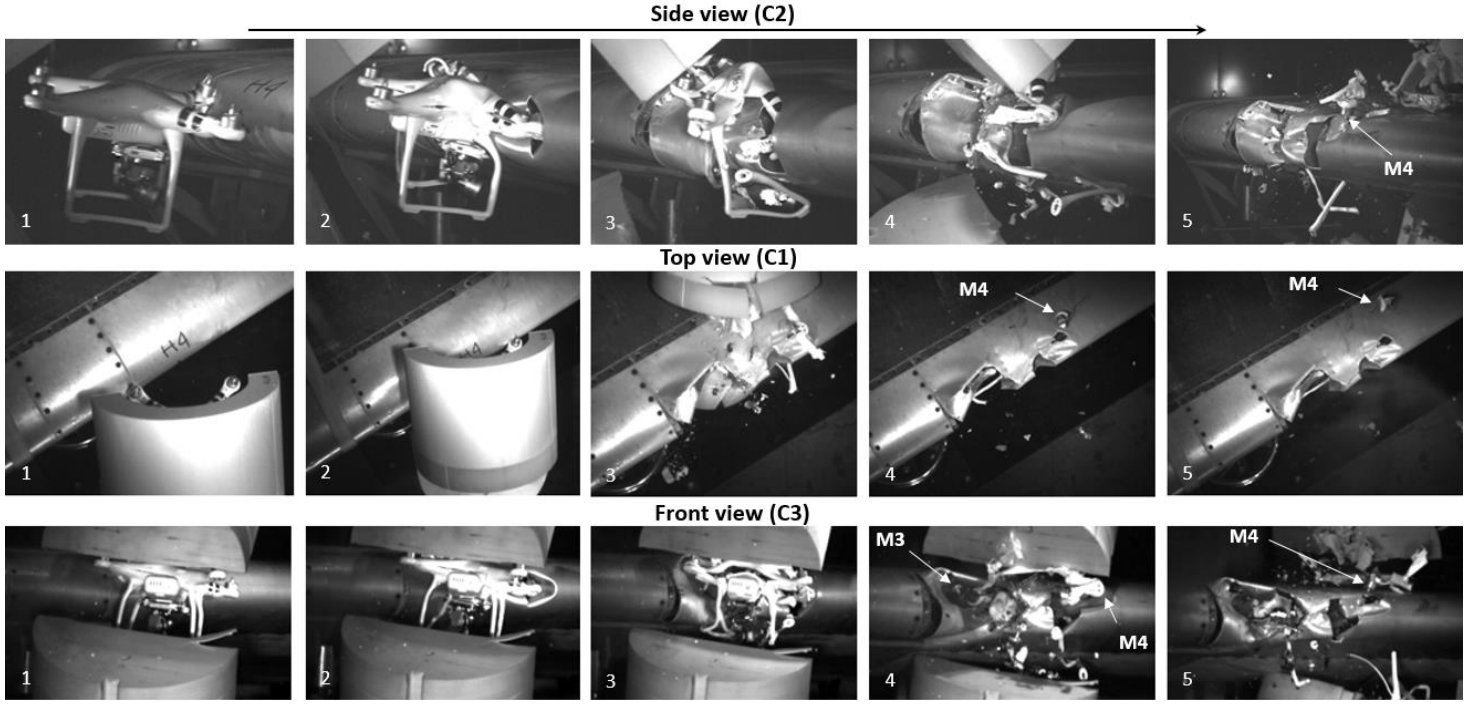

Figure 17: Drone-HS impact sequence (Test #2: HS-T2)

The impact resulted in multiple openings on the leading edge as depicted in **Figure 18**.Three out of the four motors punctured the leading edge and the skin was disjointed from the LER 15 and was severely torn. Both leading edge ribs (15 and 16) were deformed. The front spar was also deformed and bent at its top. **Figure 19** gives the main dimensions of the various openings that resulted from the impact. Parts of the test drone were found inside the HS ahead of the spar and at the back of the HS as depicted in **Figure 20**. Battery pouches overheated and failed. Their remains were found inside the HS as the figure shows.

Figure 18: Overall view and close-up of damaged areas (HS-T2)

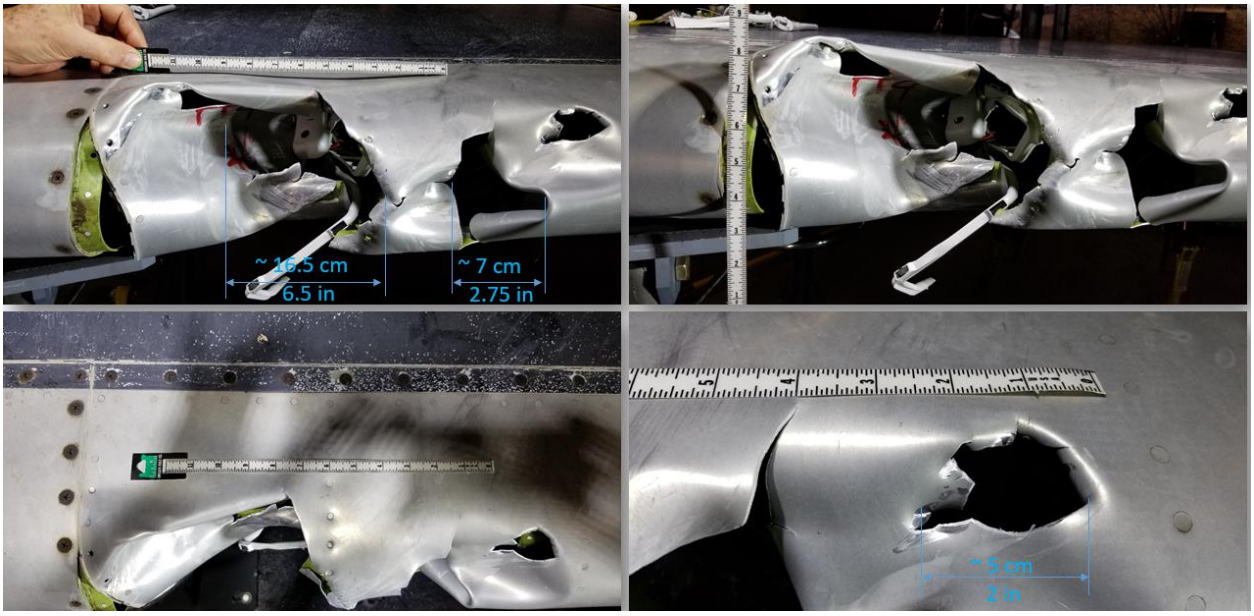

Figure 19: Main dimensions of the damaged areas (HS-T2)

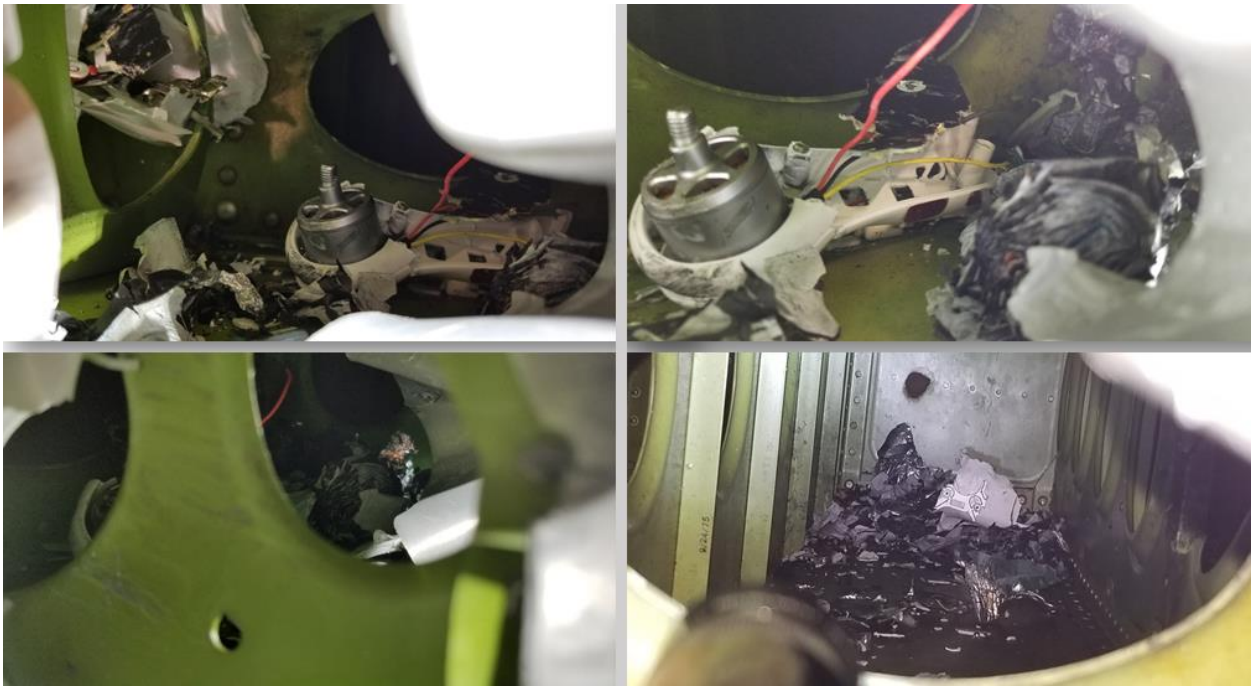

Figure 20: Remains of the test drone inside the HS (HS-T2)

3.1.3 Test #3 (HS-T3)

The third test (HS-T3) was conducted on the same HS segment at mid span between the T1 and T2 shots as shown in **Figure 21**. The stabilizer was strapped in place as depicted in the figure. Similarly to the previous two tests, target was located at the apex of the leading edge and between the LERs 20 and 21. The laser-based mechanism used in all tests to align the target points on the leading edge with the cannon is shown in **Figure 22**. This impact test featured a drone with a fully charged battery to assess the risk of fire after impact. The drone was powered-up before being loaded into the barrel. A large capacity ducted-fan was also set up and used to ventilate the test area to remove smoke and noxious fumes that may be generated from overheating of the impact-damaged battery pack.

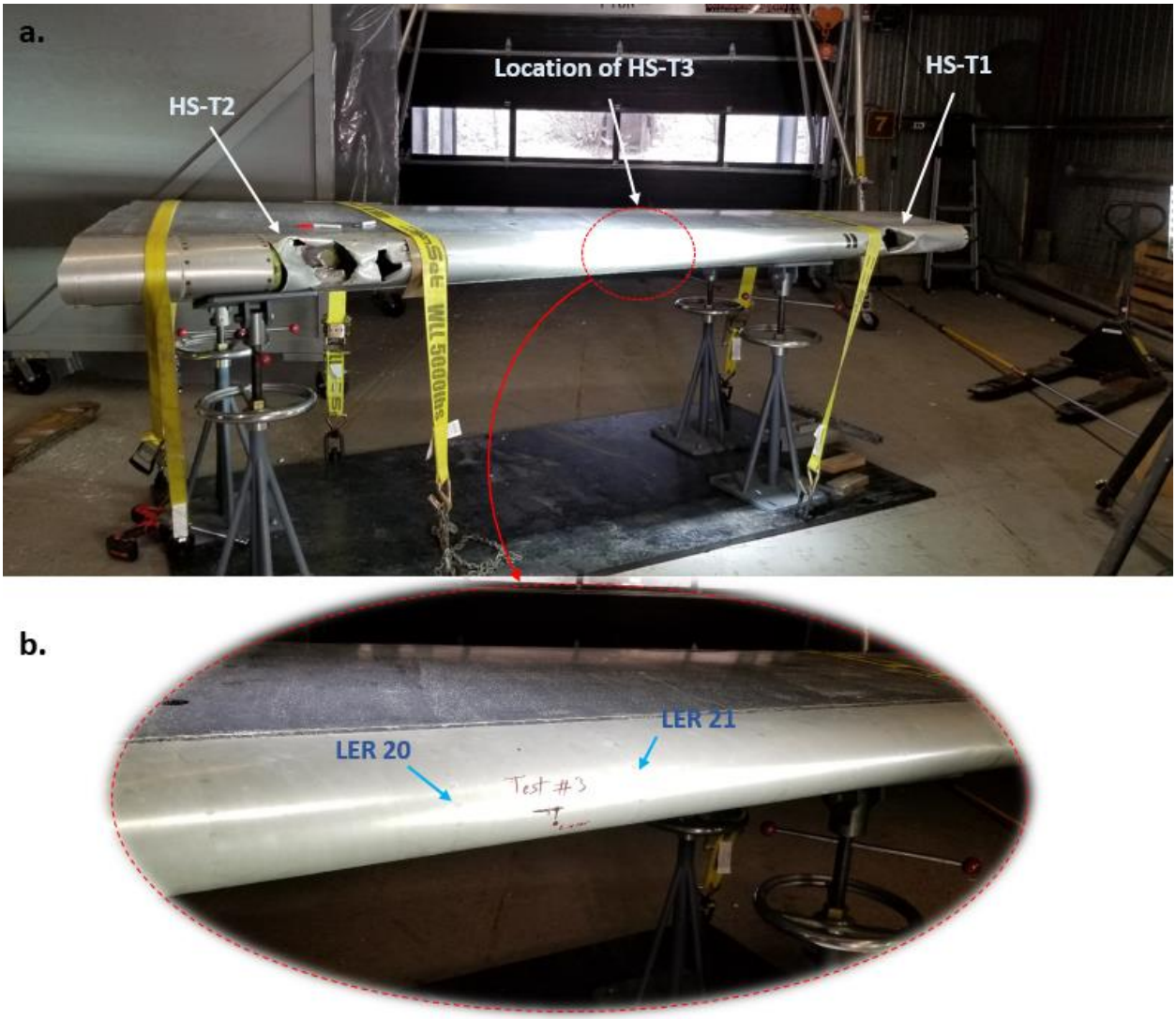

Figure 21: Setup for Test #3 (HS-T3)

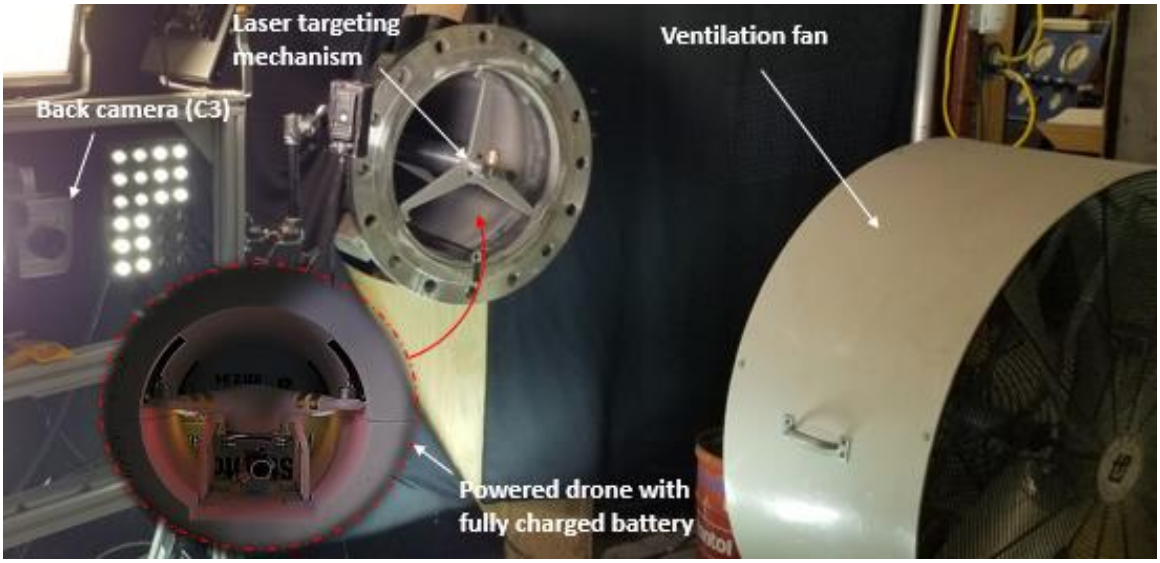

Figure 22: Test preparation (HS-T3)

Figure 23 depicts pictures of the HS segment right after the test. The shot was on target at a speed of 126.4 m/s (245.7 kt). The drone penetrated the leading edge and the impact resulted in severe damage to its structure. The impact has also caused smoke to come out through the various openings of the HS. The smoke was dense and the fan was immediately employed to clear the test room. The HS segment was quickly dismounted and moved outside of the testing facility to prevent exposure to the smoke (**Figure 24**). Based on thermal images of the HS upper skin surface of the structure adjacent to the rear spar, the temperature was 104°C (219°F) suggesting ignition of the battery cells near this location. The outdoor ambient was near freezing with a wind both of which were contributing towards cooling the structure.

It is important to note that despite activating the large-capacity fan and quick response in moving the HS segment outside of the test facility, the smoke spread throughout the facility and control room. The facility was vacated to allow for proper ventilation as exposure to such fumes may represent a serious health hazard. The project team has decided to carry subsequent tests using drones with discharged batteries only.

Figure 25 shows the impact sequence for this third test from the three camera positions. The sabot separation was slightly delayed which led to the sabot upper part obscuring the view of the impact sequence from the top camera (C1). However, the side and front cameras (C2 and C3) captured the main impact scene. As opposed to the first two tests, the drone exhibited higher yaw and roll rotation angles: 15° for the yaw and 13.5° for the roll. This could have been due to the slight weight differences between the test drones (~ 60.9 g) and mass distribution. The pitch angle was very close to that recorded for HS-T2 with a value of 7° (downward).

As a result of the drone roll angle, Motor M2 hit the leading edge under the apex at the LER 20 location. It was followed by M1 and its arm and then the drone's main body. M1 also impacted

a leading edge rib (LER 21). As the rib locations represent the stiffest points of the leading edge structure, the motors caused dents but did not penetrate: M2 featured a free fall after the impact whereas, M1 was deflected away towards the trailing edge of the horizontal stabilizer. The drone legs and M3 were the last to hit the leading edge. The drone arm containing M4 broke completely and caused the motor to divert from the leading edge. The camera module was still attached to the drone during the impact and passed under the leading edge.

Figure 23: Post-test pictures (HS-T3)

Figure 24: Test segment after impact

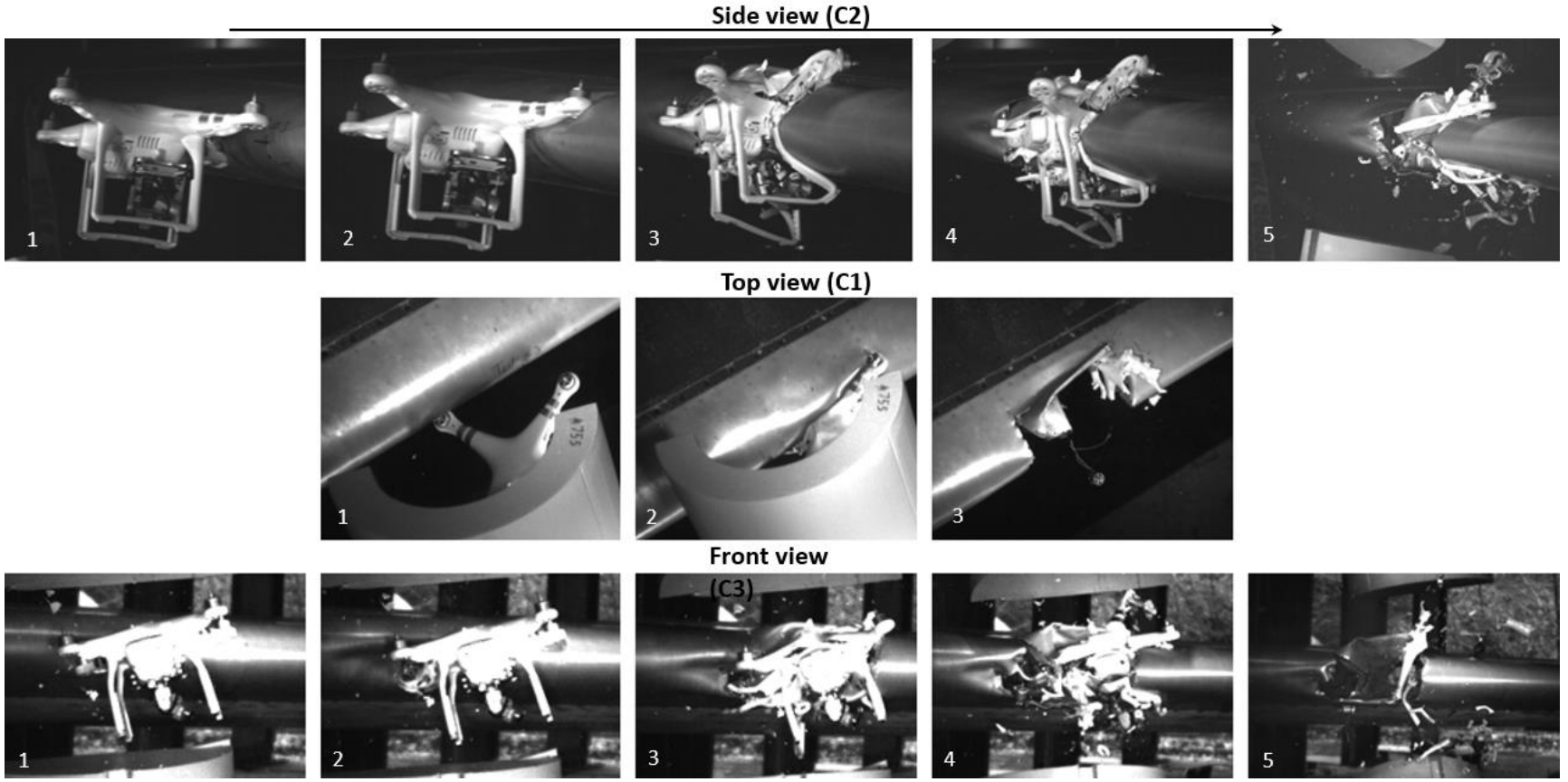

Figure 25: Drone-HS impact sequence (Test #3: HS-T3)

The damage to the leading edge structure covered the total distance between the leading edge ribs (**Figure 26**). The skin of the leading edge sheared along the rivet lines. Both LERs (20 and 21) were deformed, torn and displaced as was the front spar as depicted in **Figure 27**.

Figure 26: Damage dimension (HS-T3)

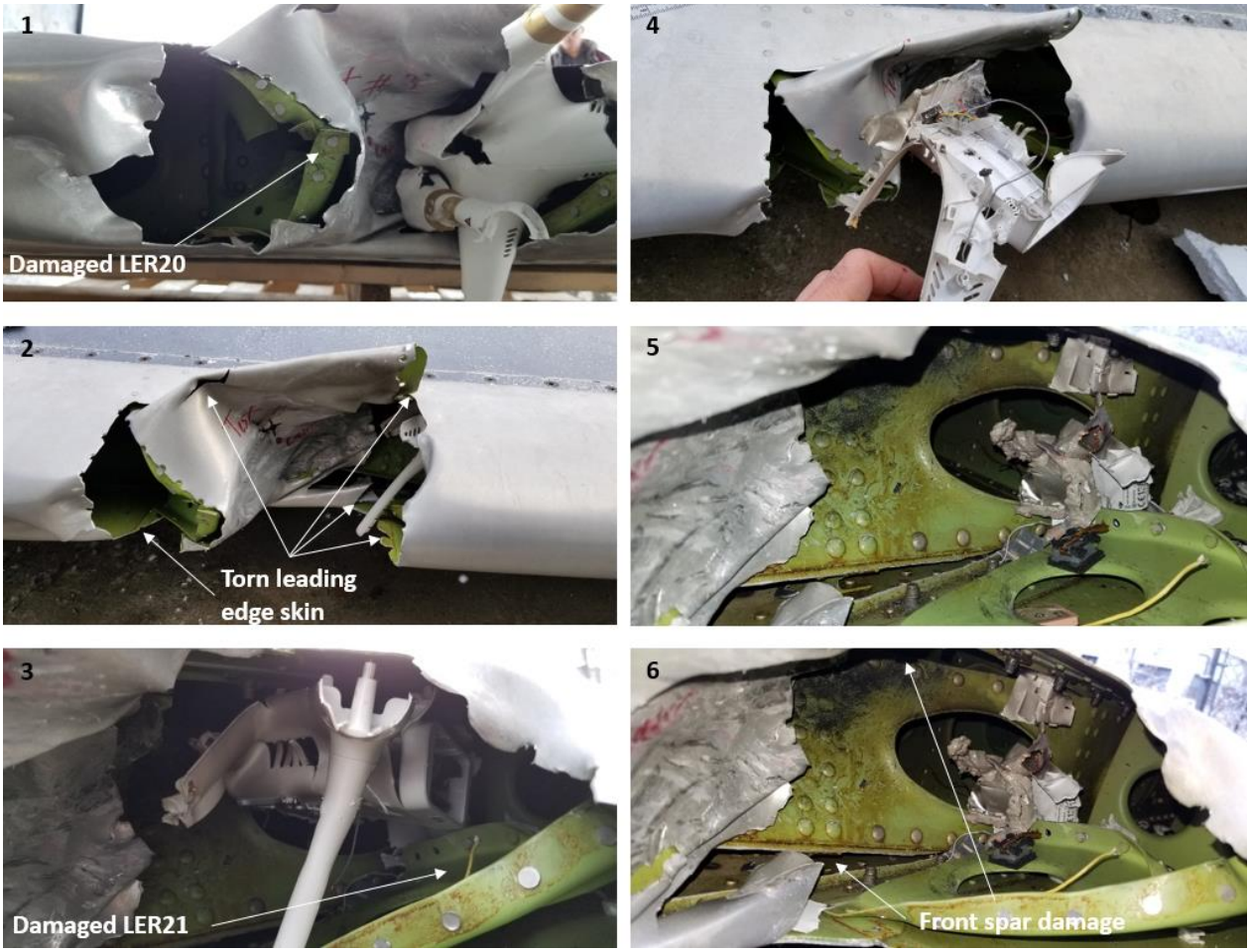

Figure 27: Damage to the leading edge structure (HS-T3)

Pieces of the drone structure were found in the opening caused by the impact (**Figure 27**) and other debris, including the remains of the burnt battery, were located at the back of the HS close to the rear spar as depicted in **Figure 28**.

Figure 28: Shattered drone structure and burnt battery debris (HS-T3)

3.1.4 Test #4 (HS-T4)

The fourth test (HS-T4) was conducted on the LHS HS (inboard portion) of the central segment as was previously indicated in **Figure 7**. The test setup is presented in **Figure 29** with a target location at mid span between LER3 and LER4. It is important to note that LER3 is stiffer and wider than LER4. This leading edge rib serves to join the fixed and removable segments of the HS leading edge. As the figure shows, four dents on the horizontal stabilizer portions are visible close to LER1 and LER6 (LHS HS) and close to LER2 (RHS HS). These dents were caused by the impact of the four drone motors from a previous test on the vertical stabilizer (VS-T1) as will be discussed in the next section.

The central segment of the empennage was properly aligned with the centerline of the cannon allowing the HS segments to be at their correct sweep angle of 40°. The drone was launched with a discharged battery. The impact was on target at a speed of 126.4 m/s (254.6 kt). This test featured a drone rotation of about 14° in all directions (pitch: 13.5°, yaw: 14° and roll: 15°). The drone hit the leading edge in the following order: M1, M2/main body, legs, M4 and finally M3 as depicted in the frames extracted from the high speed camera videos (**Figure 30**). The drone's downward pitch and clockwise roll rotations caused M1 to hit the leading edge under the apex. The motor did not penetrate the leading edge but caused a deep dent on its skin. The drone arm holding M1 broke upon collision with LER3. M2, the drone main body with battery and M4 impacted the apex of the leading edge and penetrated the HS. The arm containing M3 impacted LER3 and broke. This caused M3 to roll over, tear the leading edge skin and then deflect away from the HS. The camera module passed under the HS and did not contribute to the impact.

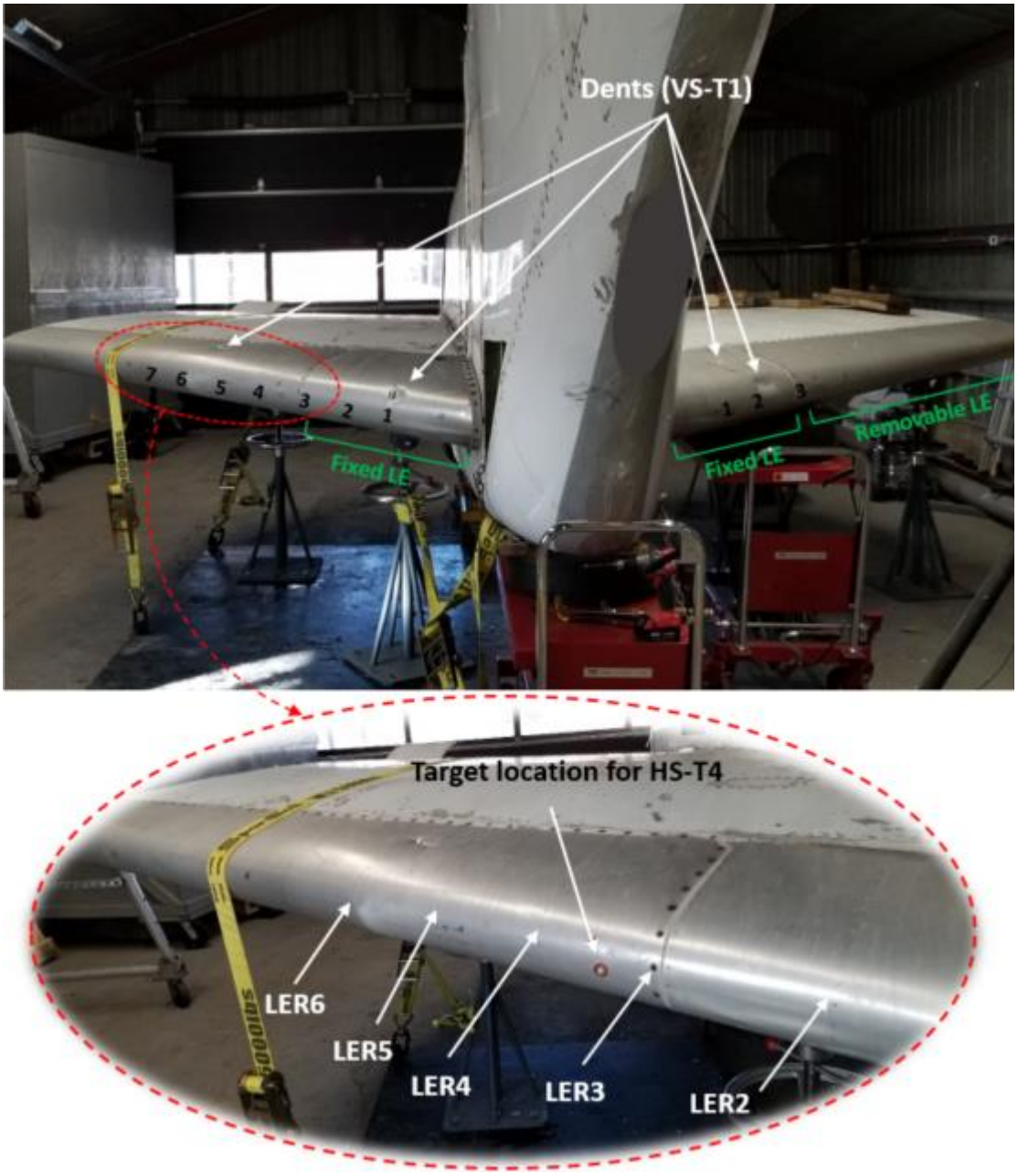

Figure 29: Test setup (HS-T4)

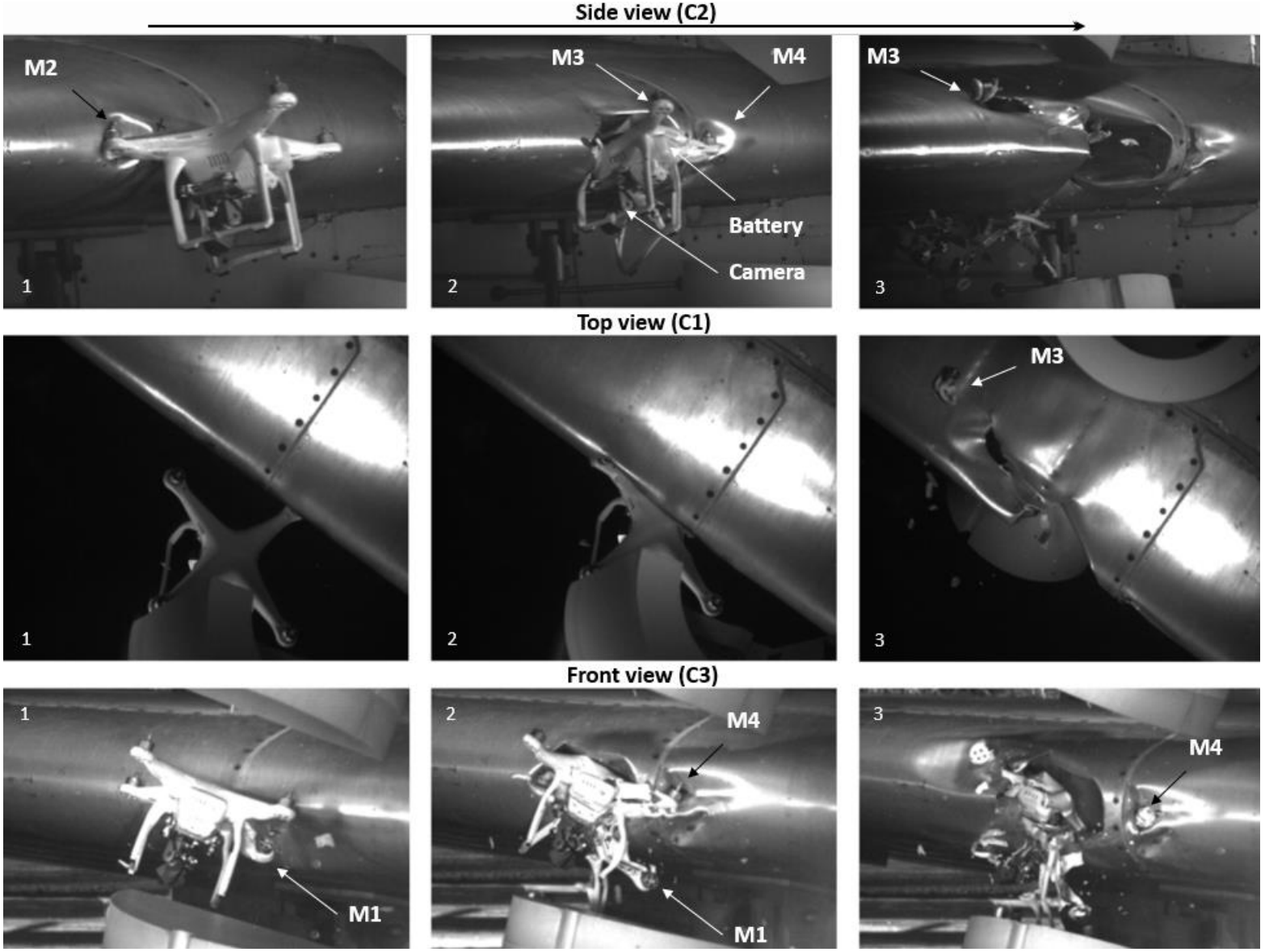

Figure 30: Impact sequence (HS-T4)

The drone impact caused damage to the leading edge that extended over a distance of 48.2 cm (19 in). The width of the damage at the centre of the impact was about 20 cm (8 in) as depicted in **Figure 31**. The impact locations of the four motors on the leading edge are indicated in **Figure 32**.

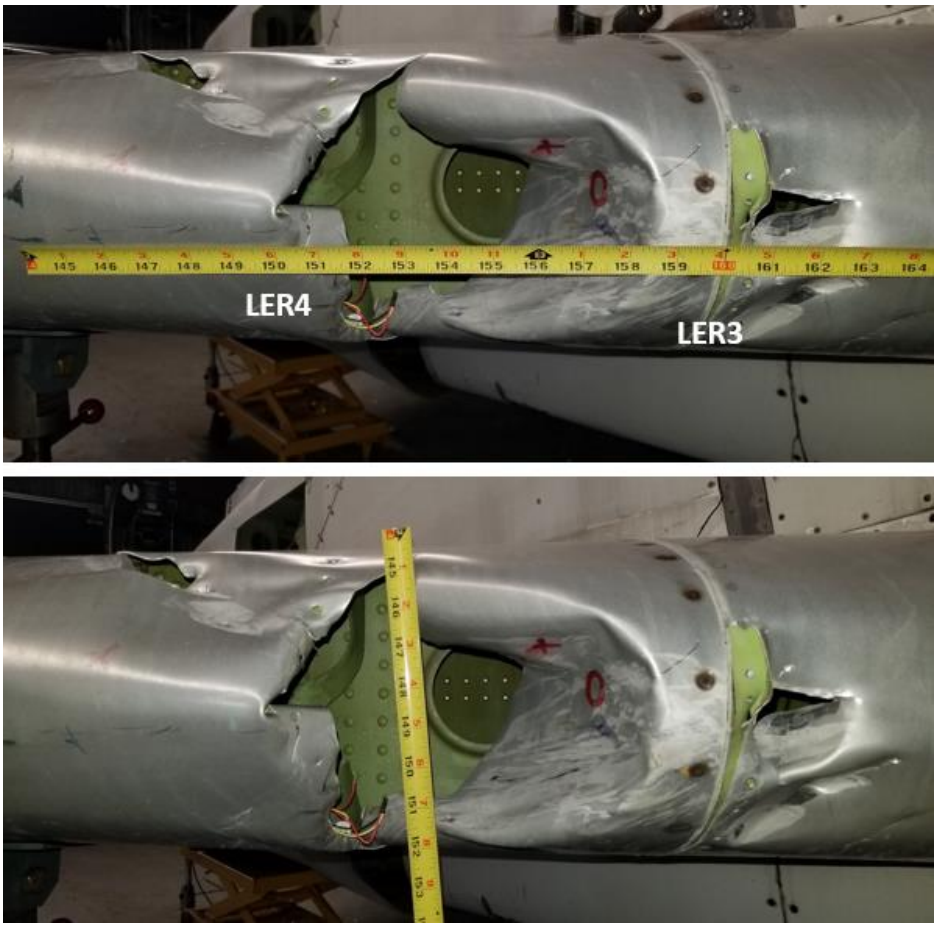

Figure 31: Damage to the leading edge structure (HS-T4)

Figure 32: Impact locations of the motors (HS-T4)

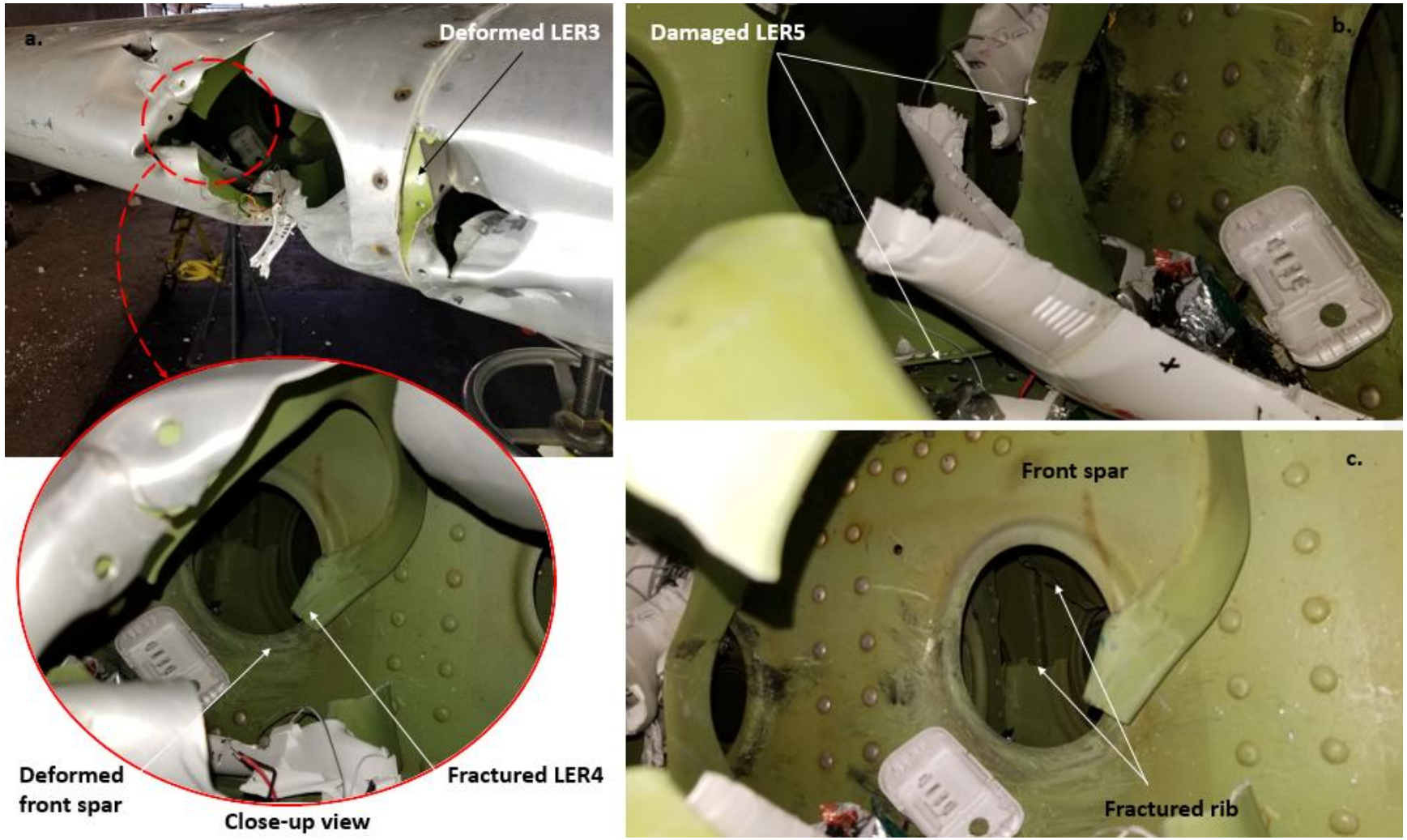

Figure 33: Damage to internal structure (HS-T4)

Figure 33 shows pictures of the damage incurred to the HS interior structure. LER3 was deformed and LER4 suffered severe damage and fractured at two locations. LER 5 was also deformed and disjointed from the lower skin surface. The front spar was also deformed in the vicinity of a lightening hole. Similarly to the previous tests, the battery pack passed through the lightening holes of the front spar, caused damage to the internal structure and landed near the rear spar of the HS. **Figure 34** shows damage to the leading edge as viewed from above (a) and debris of the drone body found inside the damaged section of the leading edge (b) as viewed from the side through the lightening holes of the LE ribs (looking inboard).

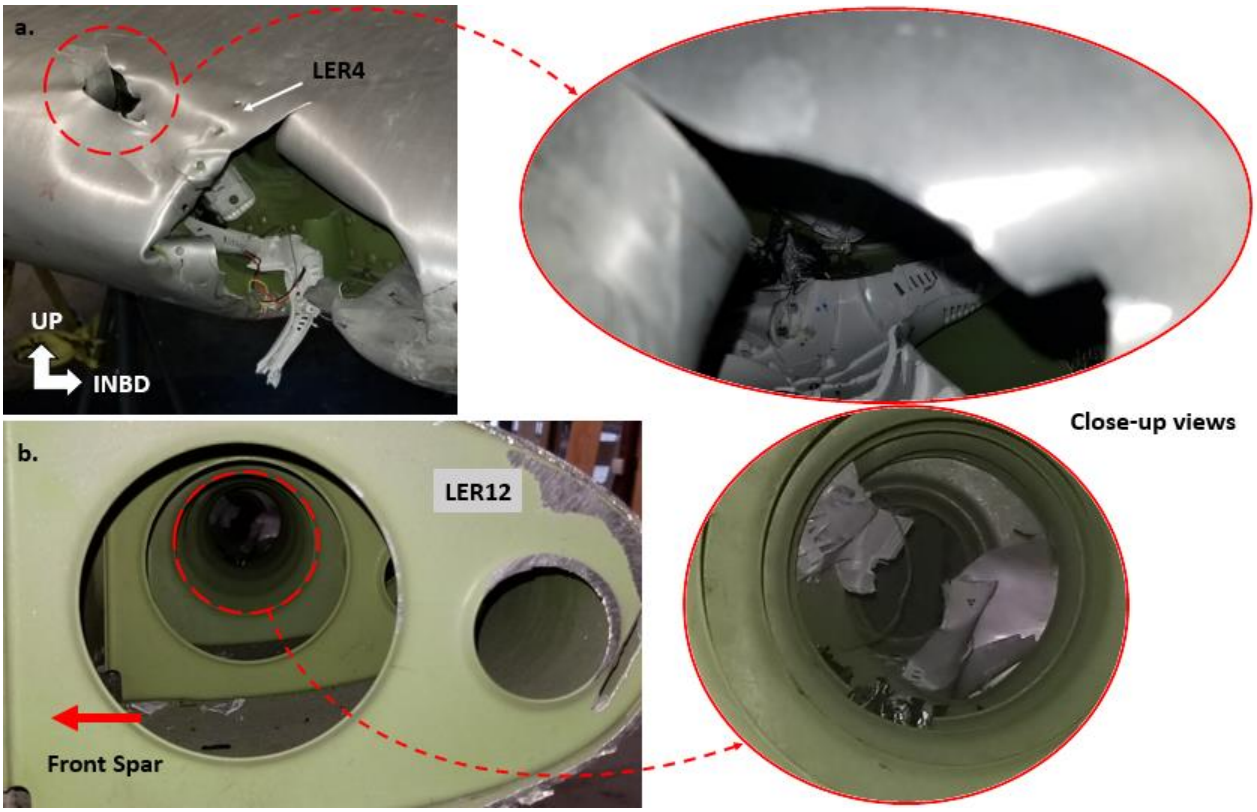

Figure 34 : Drone structural debris (HS-T4)

3.1.5 Test #5 (HS-T5)

The fifth drone impact test on the horizontal stabiliser was conducted on the same centre segment with a target point at midspan between LER7 and LER8 as shown in **Figure 35**. The drone was launched with a discharged battery.

The drone impacted the leading edge on target at a speed of 132.3 m/s (257.2 kt) and penetrated the HS. **Figure 36** shows frames of the impact sequence extracted from the high speed camera videos. Compared to the fourth test, the drone exhibited an upward pitch rotation of 9° and only a slight yaw rotation angle (2°). However, the roll angle was similar in direction (clockwise) and amplitude (16°). Motor M1 was the first to impact the leading edge close to LER7, followed by the main body/battery, legs, M2 arm, camera module, M4 and finally M3. M1 deformed the leading edge section between LER6 and LER7, pierced the skin and lodged inside the HS. Its arm broke off upon contact with LER7. The roll angle caused M2 and its arm to graze the upper surface of the leading edge skin and then deflect above the HS. The main body/battery, camera module and M4 tore and penetrated the leading edge. M3 was the last component to impact the HS. Its arm broke on contact with LER8. The motor hit the leading edge past LER8, rolled over, ripped the LE upper skin surface and then deflected away from the leading edge.

Figure 35: Test setup (HS-5)

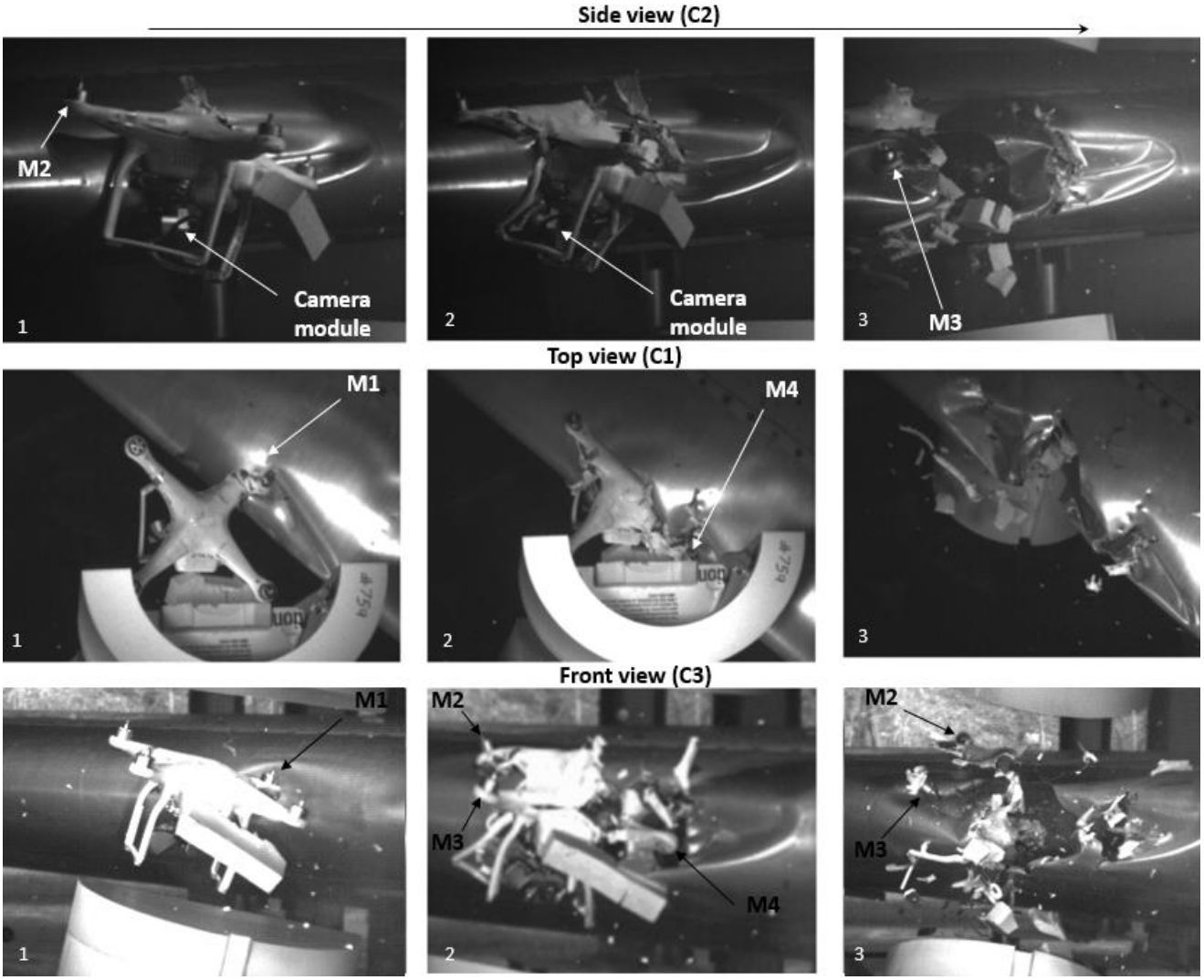

Figure 36: Impact sequence (HS-T5)

The damage to the leading edge extended from LER6 to LER 9 over a total distance of 71 cm (28 in) as shown in **Figure 37** The main penetration of the leading edge measures 15.2Wx16.5H cm (6.0Wx6.5H in). **Figure 38** identifies the drone components that caused the various damages on the leading edge skin.

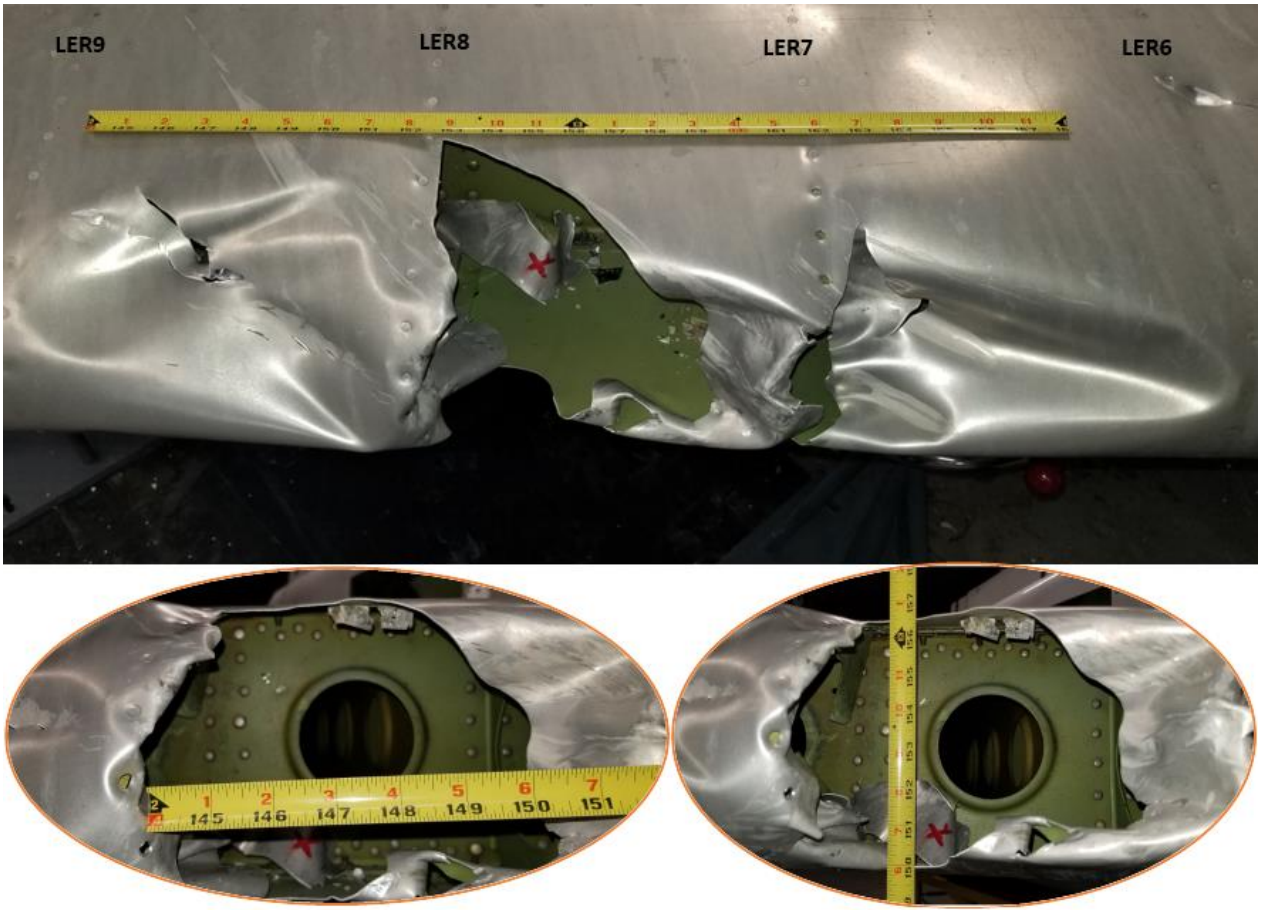

Figure 37: Damage to the leading edge structure (HS-T5)

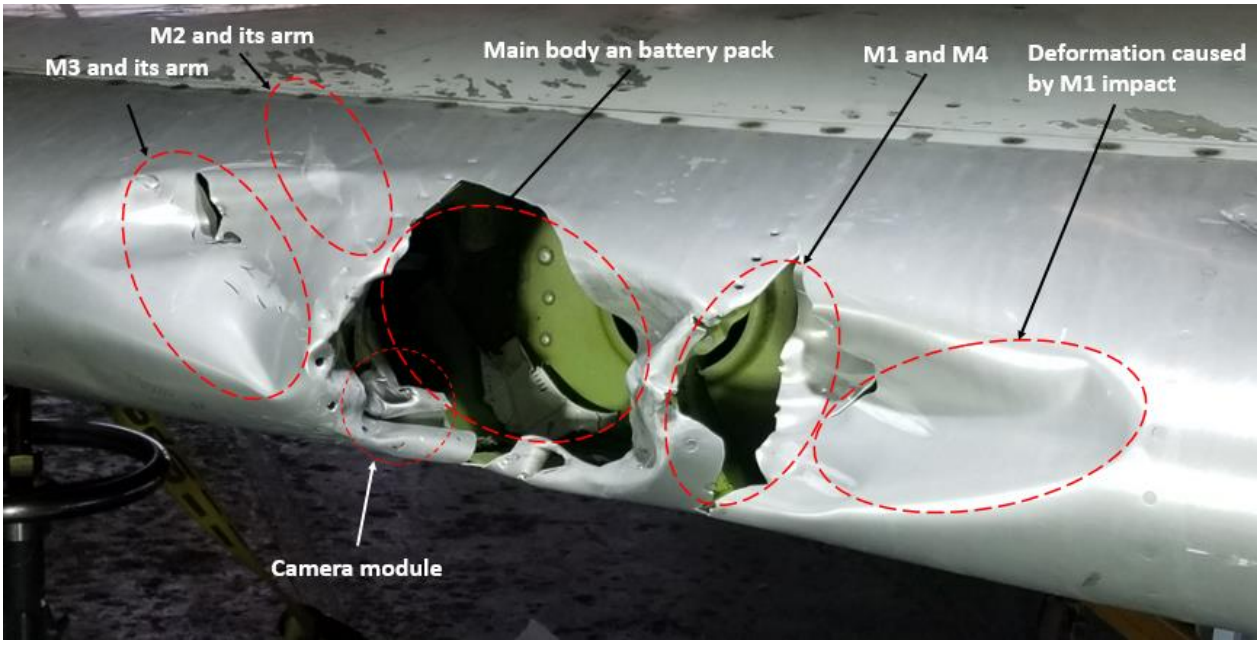

Figure 38: Impact locations of the drone components (HS-T5)

Figure 39 shows the damage caused to the internal structure of the HS. LER8 was deformed, detached from the LE skin and fractured. **Figure 40** shows the damage caused to LER 7 and the surrounding leading edge skin. Parts of the drone were found inside the HS in various locations.

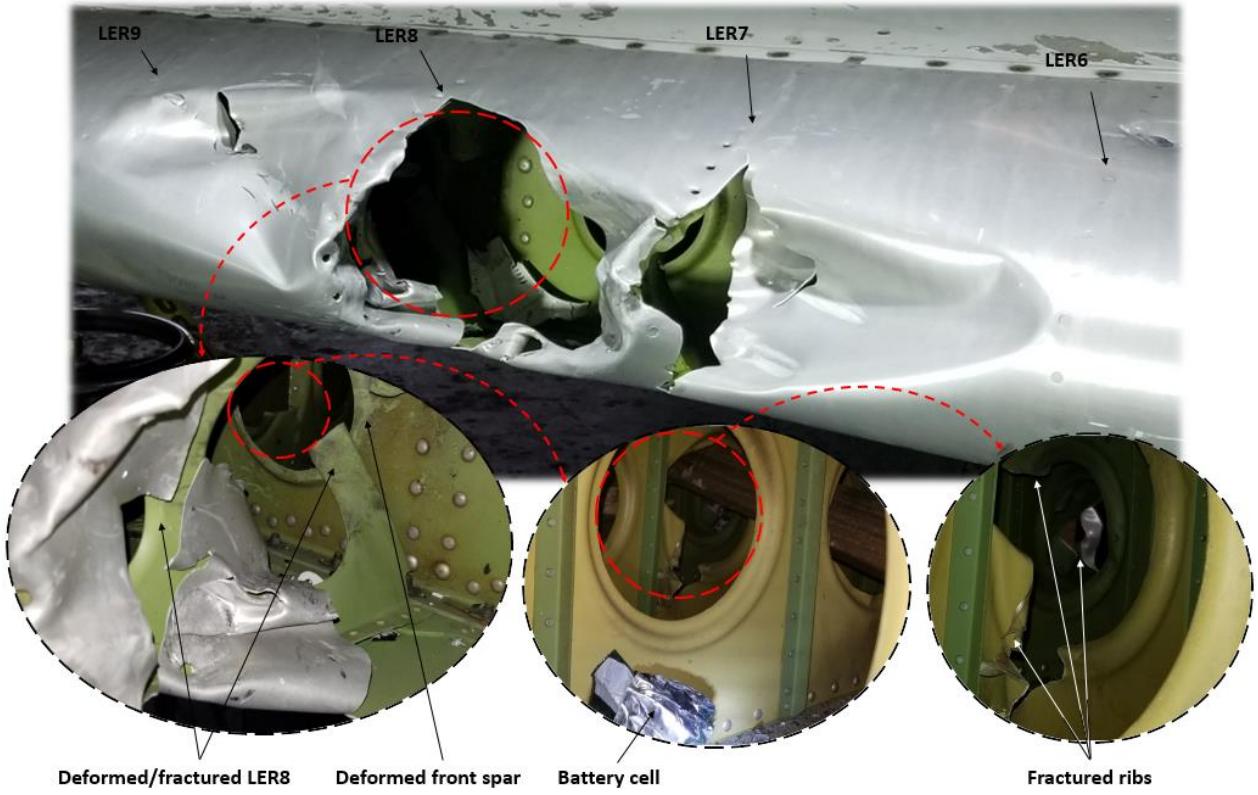

Figure 39: Damage caused to the HS internal structure (HS-T5)

Figure 40: Damage caused to LER7 and its vicinity (HS-T5)

3.2 Drone impact on vertical stabilizer

A general view of the vertical stabilizer (VS) central segment (upside down) is presented in **Figure 41**. For illustration purposes, the leading edge ribs (LER) on the upper panel have been numbered and identified with red-doted lines. The front spar on the VS is identified with a blue-dotted line. This figure also shows the fixturing setup used for the impact test (VS-T1). The central segment weighs 1312 kg (2893 lb). The VS was aligned with the centerline of the cannon and fixed to the floor. Two hydraulic lifting devices were placed and adjusted to support under each side of the HS to set it level. Two others were installed at the front of the VS and adjusted to set the layback angle of the leading edge to the correct value of 59° as previously shown in **Figure 7** and **Figure 8**. As all of the hydraulic lift units were wheeled, the segment was strapped to a steel plate on the floor to resist movement rearwards during the impact.

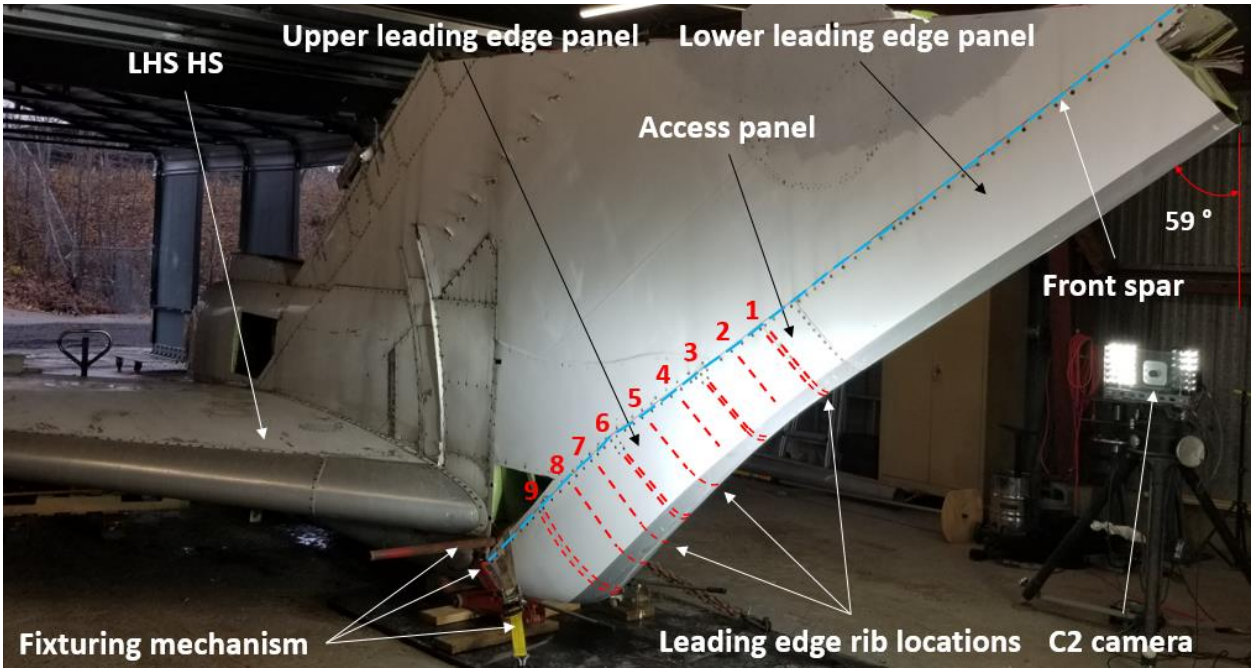

Figure 41: Vertical stabilizer

It is important to note that the structure and size of the ribs vary depending on their location and structural functionality. **Figure 42** shows an inner picture of the leading edge viewed from its exposed side of the lower panel (**Figure 41**). The LERs can be categorised as either single or composed. The single ribs are mounted to the leading skin with a single row of rivets on each side of the rib as depicted in **Figure 43**. The apex area of the leading edge is not supported by the rib. However, the composed ribs provide full support to the leading edge internal surface. **Figure 44** depicts a composed LER mounted to the leading edge with a single-row of rivets. On the other hand, **Figure 45** shows partial pictures of composed ribs assembled to the leading edge with a double-row of rivets. The structure of the latter ribs may also differ as the figure shows.

Figure 42: Leading edge inner structure

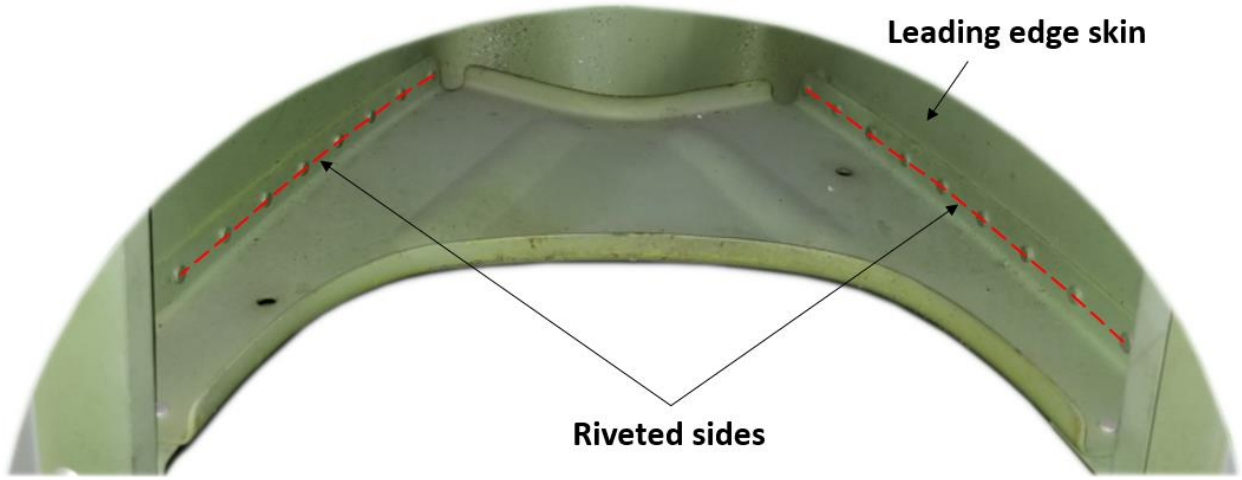

Figure 43: Single leading edge rib

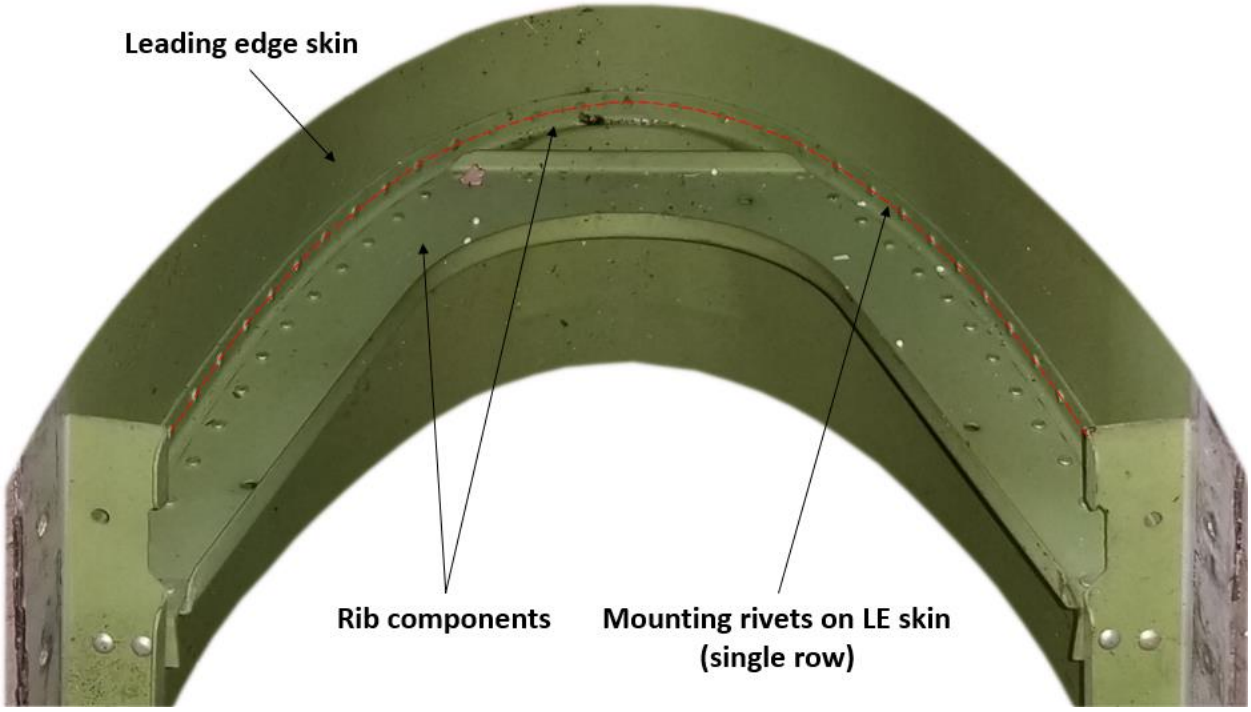

Figure 44: Composed leading edge rib (single-row rivets)

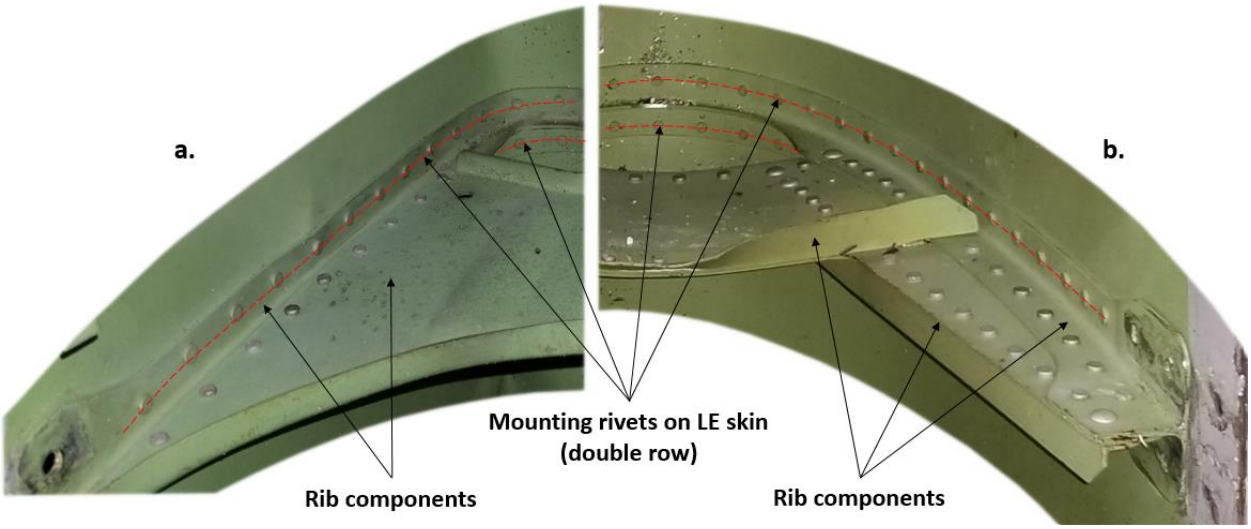

Figure 45: Composed leading edge rib (double-row rivets)

3.2.1 Test #6 (VS-T1)

The target for the vertical stabilizer test (VS-T1) was located between LER2 and LER3. The former is a single rib whereas, the latter is a composed rib mounted to the LE with a double row of rivets (**Figure 45a**). **Figure 46** shows the test setup for VS-T1.

The drone hit the leading edge on target, closer to LER2, at a speed of 130.7 m/s (254.1 kt). The impact caused a tear in the leading edge skin without penetration by any of the drone components. **Figure 47** shows frames of the impact sequence extracted from the high speed camera videos located at the side (C2) and front (C3) of the test segment. The orientation of the test segment with the layback angle of 59° obscured the view of the impact sequence from the top camera (C1). As the images show, the main body of the drone impacted the leading edge of the VS with an upward pitch angle of 9.5° and a counter clockwise roll angle of 9°. The motors of the drone missed the leading edge due to its parabolic curvature and the orientation of the VS. The arms of the motors broke off upon impact with the LE and were deflected to the sides of the VS. As a result, the motors impacted the inboard segments of the horizontal stabilizers and caused collateral damage as depicted in **Figure 48** and **Figure 49**. The collateral damage on the HS segments was not very significant as one can notice. The trajectory of the motors could also be different in a real case due to the air flow, which was not considered for this test.

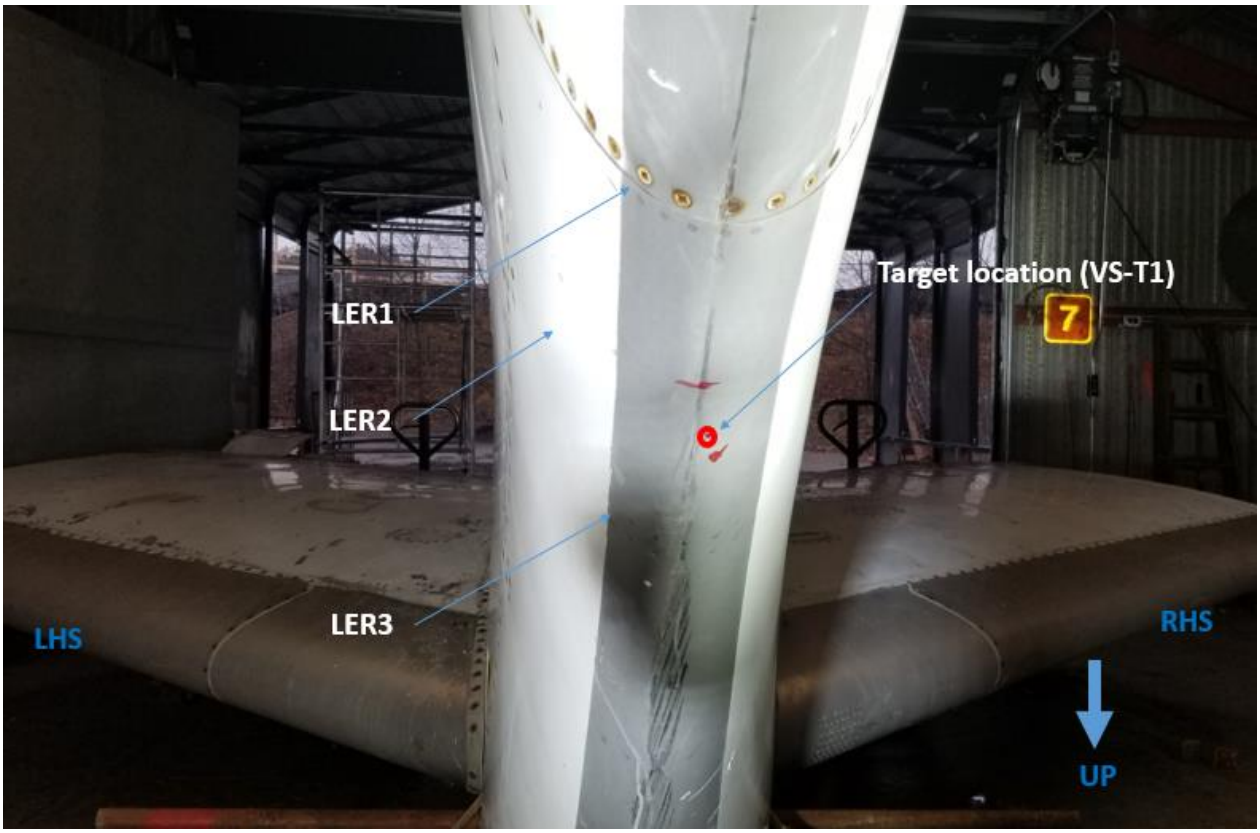

Figure 46: Test setup (VS-T1)

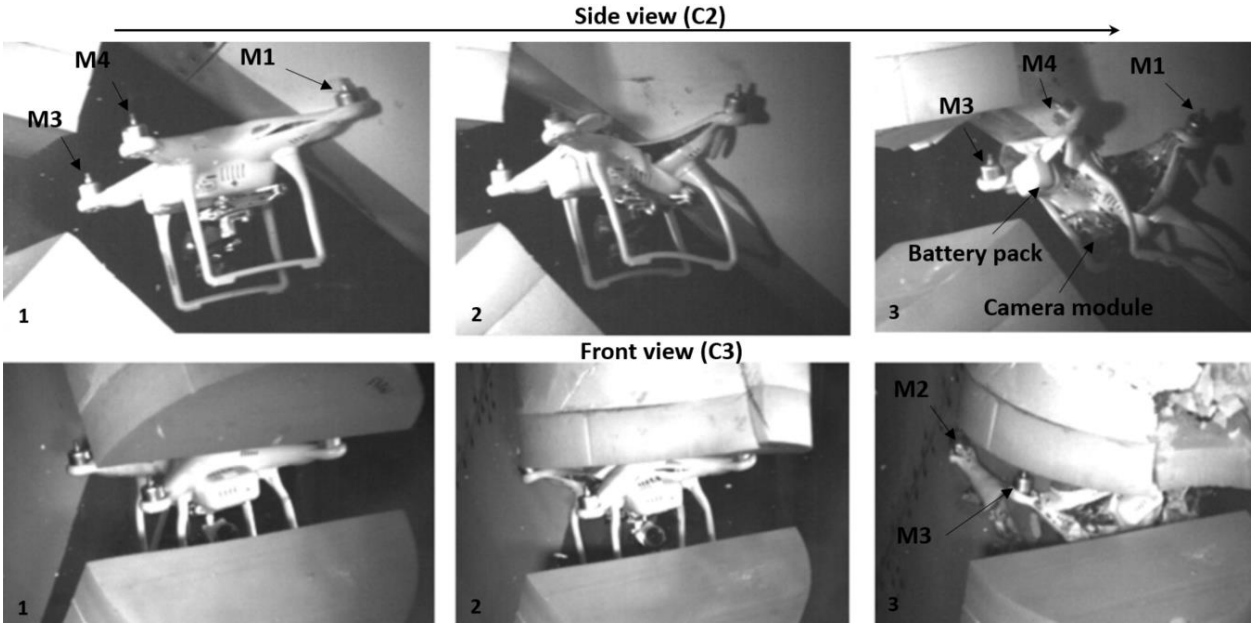

Figure 47: Impact sequence (VS-T1)

Figure 48: Collateral damage on RHS HS (VS-T1)

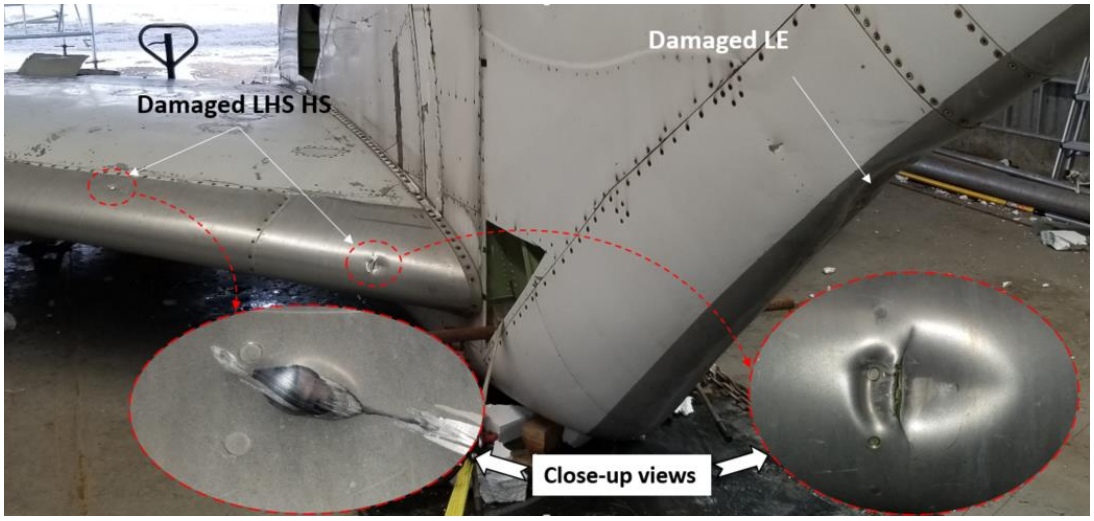

Figure 49: Collateral damage on LHS HS (VS-T1)

The damage on the VS leading edge extended over a distance of about 30 cm (11.8 in) and was more pronounced on one side of the LE where the rivets failed and the skin was partially disjointed from the LERs 2 and 3 (**Figure 50**). As opposed to the drone impact on the HS, the VS withstood the impact and no penetration was reported. The impact caused a permanent deformation and tears on the LE skin. It is worth noting that motors M1 and M2 grazed both sides of the VS leading edge as they were deflected away after the impact (b and c).

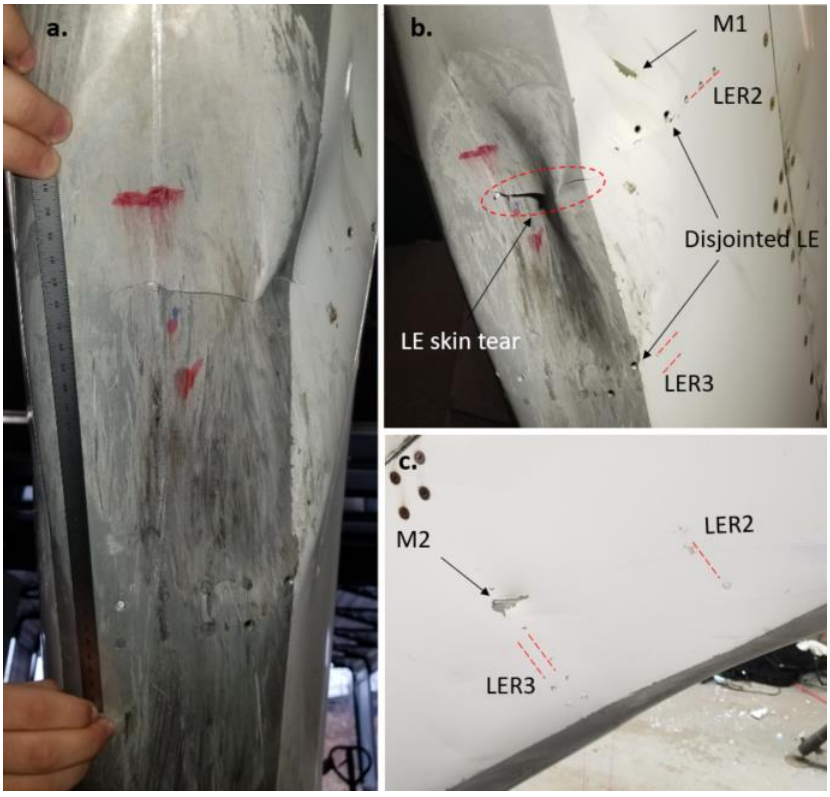

Figure 50: Damage to the leading edge structure (VS-T1)

The access panel was removed to allow inspection of the interior of the leading edge. **Figure 51** clearly shows the tear on the leading edge skin as well deformation and partial fracture to LER3.

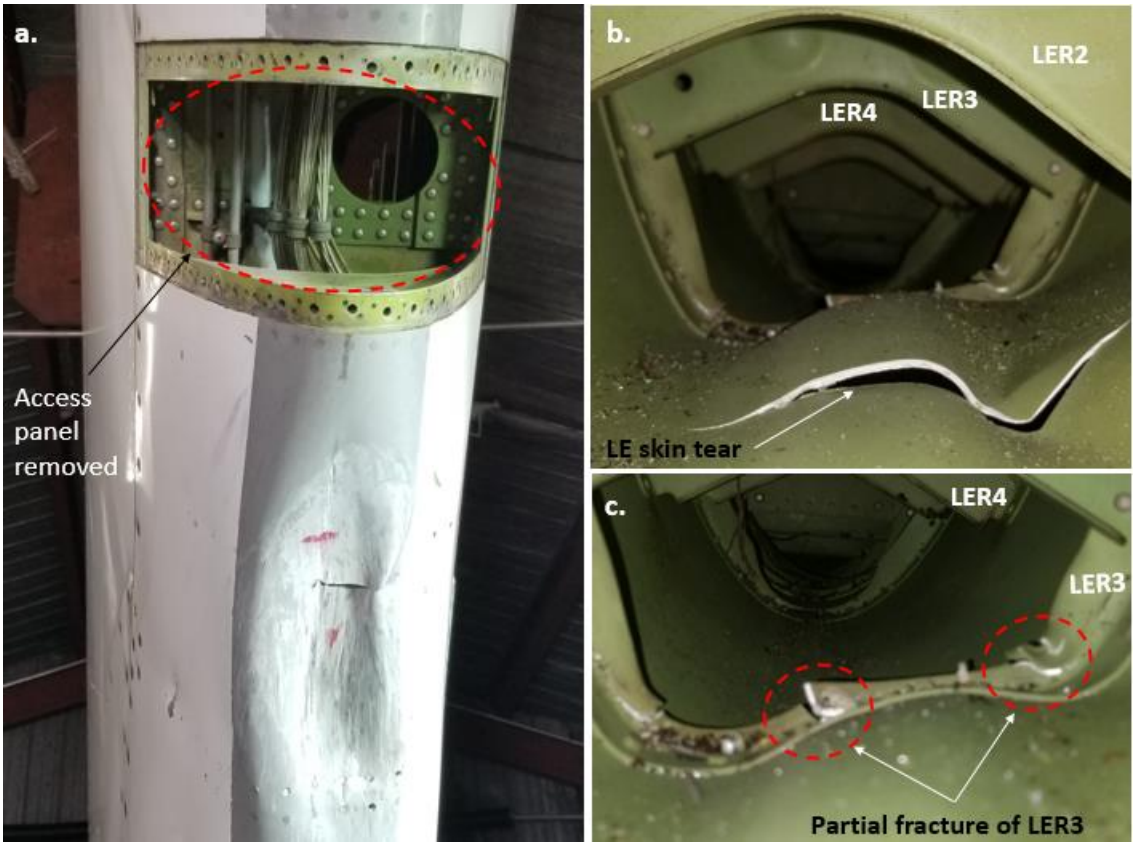

Figure 51: Damage caused to the VS internal structure (VS-T1)

3.3 Bird impact on horizontal stabilizer

A bird impact test (HS-T6) on the outboard segment of the RHS was performed to compare the damage severity level with the impact tests performed using the quadcopters on the LHS segment. The bird weight was in the same range of the quadcopters and another pneumatic cannon (bore of 15.2 cm, 6 in) and sabot support system was used to launch the bird package for this test. ASTM standard F330-16 was used as a guideline for the bird impact. **Figure 52** shows a general view of the pneumatic cannon and **Figure 53** depicts the test segment setup. As the figure shows, four adjustable stands and three hydraulic lift tables were used to support the leading edge of the horizontal stabilizer with the target location aligned with the centerline of the cannon. The test segment was fixtured and restrained with ratchet straps similarly to Test #3 (HS-T3) and the target was at mid span between LER20 and LER21. The sweep angle was also similar to that of Test #3 and was set to 32°.

Figure 52: Pneumatic cannon for bird impact (HS-T6)

Figure 53: Bird impact test configuration (HS-T6)

The bird impact was on target at a speed of 128.4 m/s (249.5 kt). The bird penetrated the leading edge of the HS and caused permanent damage as shown in the impact sequence images extracted from the high speed cameras C1, C2 and C3 (**Figure 54**). The damage extended over a distance of 24.5 cm (9.6 in) between the leading edge ribs as shown in **Figure 55**.

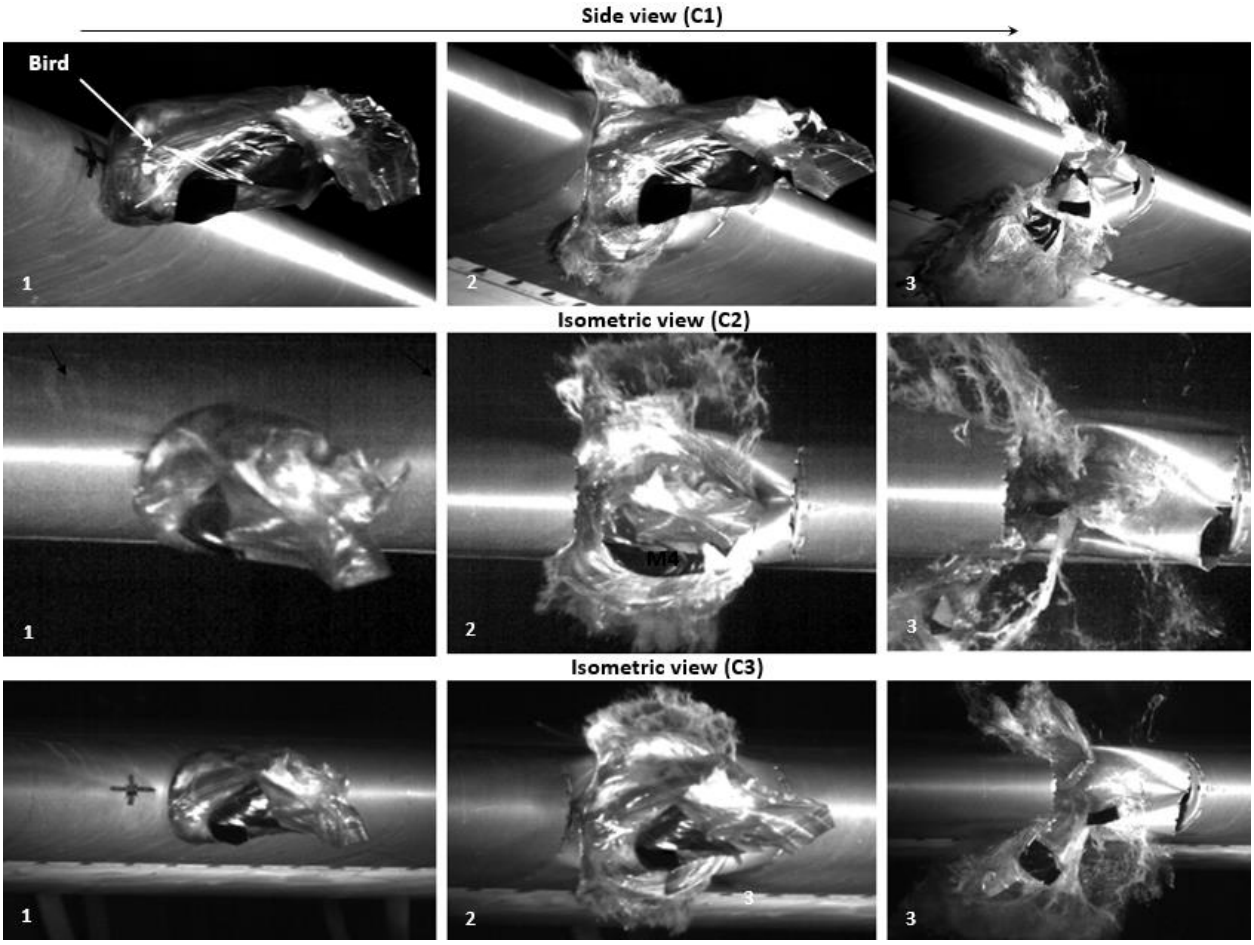

Figure 54: Selected high speed camera frames of bird impact (HS-T6)

Figure 55: Damage length on the leading edge (HS-T6)

Figure 56 presents pictures of the various HS parts that were damaged by the bird strike. The whole leading edge skin section extending from LER20 and LER21 was damaged. The leading edge skin was torn at the mounting rivets with the ribs. LER21 was fractured and dislocated from the LE skin. The front spar was also deformed and fractured. No damage to any structure located behind the front spar was reported.

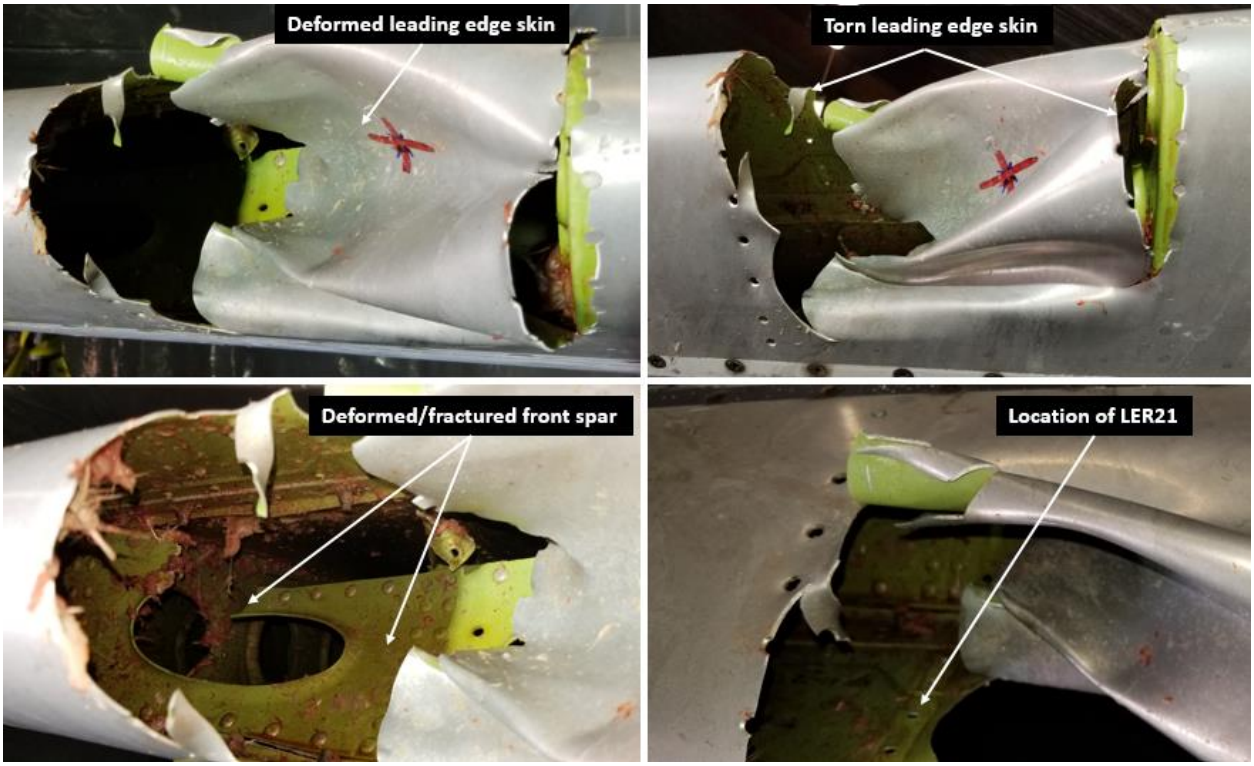

Figure 56: Damage to the RHS HS leading edge structure (HS-T6)

3.4 Data summary

A total of seven tests were conducted on the empennage of a transport category aircraft at a nominal speed of 128.36 m/s (250 kt). Seven impact tests were conducted using quadcopter-type drones and one using a bird carcass. Six out of the seven drone impacts resulted in penetration into the leading edge. The bird impact also resulted in a penetration.

The five drone impact tests on the horizontal stabilizer (various locations) caused damage to the leading edge skin, leading edge ribs, front spar as well as the stabiliser box section ribs. Drone debris, including disassociated and damaged battery cells were found close to the rear spar after the impact. The one test conducted with a fully-charged battery resulted in the battery cells overheating and igniting.

The impact tests on the vertical stabilizer caused a plastic deformation and tear to the leading edge. One of the leading edge ribs was also partially fractured. No penetration was reported for this test.

Comparing the damage severity level between the horizontal and vertical stabilizer is difficult as the internal structural support configuration and skin thickness of the leading edges are different. The VS leading edge skin is nominally 28% thicker than the HS skin (0.07 vs 0.05 in). The HS has a single LER form differing only in size depending on location along the tapered span. However, the VS employs three configurations of LER structures depending on location as was detailed above.

It is also worth noting that the damage incurred to a wing leading edge, reported in a previous study [2], was less significant compared to that on the horizontal stabilizer at the same impact speed. The difference in structure of both segments is shown in **Figure 57** and explains the difference in damage severity as a result of drone impact.

The bird impact on the HS resulted in a penetration. However, no damage to the rear parts of the HS was reported as opposed to the drone impacts that resulted in rib deformation/fracture. The weight of the bird was adjusted to be equivalent and thus directly comparable to the mass of the drone.

Figure 57: Leading edge of HS vs. wing

A summary of test conditions are presented in **Table 3**, with test data summarized in **Table 4**. In the latter, the roll angle was not reported for VS-T1 due to top high-speed camera obstruction by the vertical stabilizer. The kinetic energy at impact for each test is also presented in the table.

In addition, the FAA's Centre of Excellence for UAS Research ASSURE [5] developed evaluation criteria for airborne collisions based on over 140 impact scenarios. The analysis of the results allowed the definition of four damage severity categories as presented in **Table 5**. The latter was used as a guideline, in this study, to categorize the level of damage for each test as outlined in **Table 6**.

Table 3. Summary of impact test plan

Test ID	Velocity		Test segment	Impact location on segment	Battery charge status
	knots	m/s			
HS-T1	250 (±5)	128.6 (±2.5)	HS Outboard	LHS HS, LER25-LER26	Discharged
HS-T2	250 (±5)	128.6 (±2.5)	HS Outboard	LHS HS, LER15-LER16	Discharged
HS-T3	250 (±5)	128.6 (±2.5)	HS Outboard	LHS HS, LER20-LER21	Charged
HS-T4	250 (±5)	128.6 (±2.5)	HS Inboard	LHS HS, LER3-LER4	Discharged
HS-T5	250 (±5)	128.6 (±2.5)	HS Inboard	LHS HS, LER7-LER8	Discharged
VS-T1	250 (±5)	128.6 (±2.5)	VS	VS, LER2-LER3	Discharged
HS-T6	250 (±5)	128.6 (±2.5)	HS Outboard	RHS HS, LER20-LER21	N/A

Table 4. Summary of drone measured velocity, kinetic energy and orientation angles

Test ID	Weight		Velocity		Kinetic energy		Orientation angle [°]		
	g	lb	m/s	knots	J	ft*lbf	Pitch	Yaw	Roll
HS-T1	1177	2.59	128.2	249.2	9672.1	7120.4	18	5.5	< 2
HS-T2	1140	2.51	126.4	245.7	9106.9	6708.2	9.5	5.5	5
HS-T3	1238	2.73	126.4	245.7	9889.7	7296.2	7	15	13.5
HS-T4	1238	2.73	131.0	254.6	10622.7	7837.2	13.5	14	15
HS-T5	1241	2.74	132.3	257.2	10860.8	8024.1	9	2	16
VS-T1	1170	2.58	130.7	254.1	9993.2	7372.2	9.5	9	-
HS-T6	1254	2.76	128.4	249.5	10337.1	7613.0	N/A	N/A	N/A

Table 5. Damage level categories (FAA-ASSURE)

Severity	Description	Example
Level 1	• Airframe undamaged. • Small deformations.	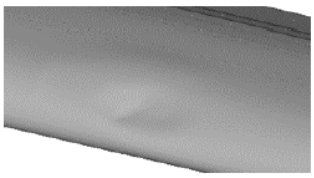
Level 2	• Extensive permanent deformation on external surfaces. • Some deformation in internal structure. • No failure of skin.	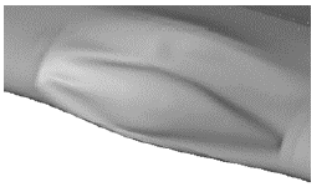
Level 3	• Skin fracture. • Penetration of at least one component into the airframe.	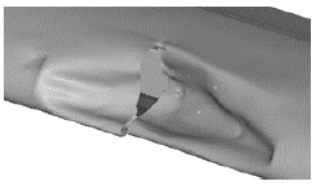
Level 4	• Penetration of UAS into airframe. • Failure of parts of the primary structure.	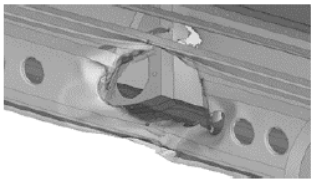

Table 6. Damage severity level

Test ID, speed (kt)	Severity	Selected damage pictures	
HS-T1, 250	Level 4		
HS-T2, 250	Level 4		
HS-T3, 250	Level 4		
HS-T4, 250	Level 4		
HS-T5, 250	Level 4		
VS-T1, 250	Level 3		
HS-T6, 250	Level 4		

4 CONCLUSION

Impact tests of quadcopter drones and bird carcass against a legacy aircraft empennage have been carried out at the National Research Council of Canada (NRC). The test campaign focused on impacting the leading edge of the vertical and horizontal stabilizers at a nominal speed of 128.3 m/s (250 kt). The latter represents the maximum operational speed allowed by the regulation for this aircraft category under 3,048 meters (10,000 feet) altitude [6]. **Table 7** provides a high level summary of the results and below is a list of the main conclusions:

- Drone impact on horizontal stabilizers results in a considerable damage to the leading edge structure, leading edge ribs, front spar and stabilizer box ribs. The damage extent and severity depends on the segment of the leading edge and orientation of the drone.
- Drone impact on vertical stabilizers causes damage to the leading edge and internal structure of the VS. The severity depends on the location of the impact on the leading edge and sub-structure design (type of LERs).
- The bird carcass impact on a segment of HS caused damage to the leading edge and internal structure of the HS visually-equivalent to that inflicted by a drone of ta similar weight. However, this observation cannot be generalized without conducting additional testing.
- The variations in pitch, roll and yaw angles of the quadcopter in combination with the thickness of the airfoil had an effect on the damage severity and its extent over the leading edge as motors and camera modules passed over and under without making contact or contributing their mass to the impact. However, these components do contribute to the impact (kinetic) energy as long as they remain attached to the drone during the initial contact with the target.
- All impact tests on the HS resulted in drone and bird penetration within the HS structure regardless of the sweep angle (32° and 40°). The test on the VS (VS-T1) caused deformation and tear to the leading edge skin as well as a partial fracture to one of the LERs.
- All impacts regardless of the state of charge of the batteries resulted in batteries cell failures.
- A penetration with a fully charged battery through a leading edge structure may represent a fire risk as the ignition of the battery may cause damage to any electrical and hydraulic systems.
- Additional testing along with simulations and analysis are needed to accurately assess damage severity and its effect on key systems/mechanisms within the empennage structure. Such work should be conducted on bird-certified aircraft components and damage severity should be assessed based on whether the aircraft is capable to successfully complete its flight during such an event or not.

Table 7. Results summary for empennage impact tests

	Legacy Transport Aircraft						
	Horizontal stabilizer						**Vertical stabilizer**
	Quadcopter					Bird	Quadcopter
Test ID	HS-T1	HS-T2	HS-T3	HS-T4	HS-T5	HS-T6	VS-T1
Severity	Level 4	Level 4	Level 4	Level 4	Level 4	Level 4	Level 3
Battery charge level	<25%	<25%	100%	<25%	<25%	N/A	<25%
Fire risk	Low	Low	High	Low	Low	N/A	Low

5 REFERENCES

[1] A. Dadouche, B. Galeote, T. Breithaupt, A. Greer, D. Backman, G. Linxi, R. Gould and C. Vidal "*Drone Impact Assessment on Flat Plates: Experimental Results*", CR-GTL-2020-0053. https://nrc-publications.canada.ca/eng/view/ft/?id=9d4ecd38-e032-4f73-80f1-51b77e0aa679

[2] A. Dadouche, B. Galeote, T. Breithaupt, A. Greer, R. Gould and C. Vidal "*Drone Impact Assessment on Aircraft Structure: Windshield and Wing Leading Edge*", CR-GTL-2020-0054. https://nrc-publications.canada.ca/eng/view/ft/?id=28f1d264-a3c2-449b-bbc1-39747f58e632

[3] ASTM F330-16, "Standard Test Method for Bird Impact Testing of Aerospace Transparent Enclosures", standard by ASTM International, 04/01/2016.

[4] https://www.ecfr.gov/current/title-14/chapter-I/subchapter-F/part-91/subpart-B/subject-group-ECFRe4c59b5f5506932/section-91.117

[5] https://www.assureuas.org/projects/completed/a3/Volume%20I%20-%20UAS%20Airborne%20Collision%20Severity%20Evaluation%20-%20Structural%20Evaluation.pdf

[i] BAAT: Stands for the names of NRC staff who designed the sabot (**B**rian, **A**llan, **A**zzedine and **T**im)